Clemson University
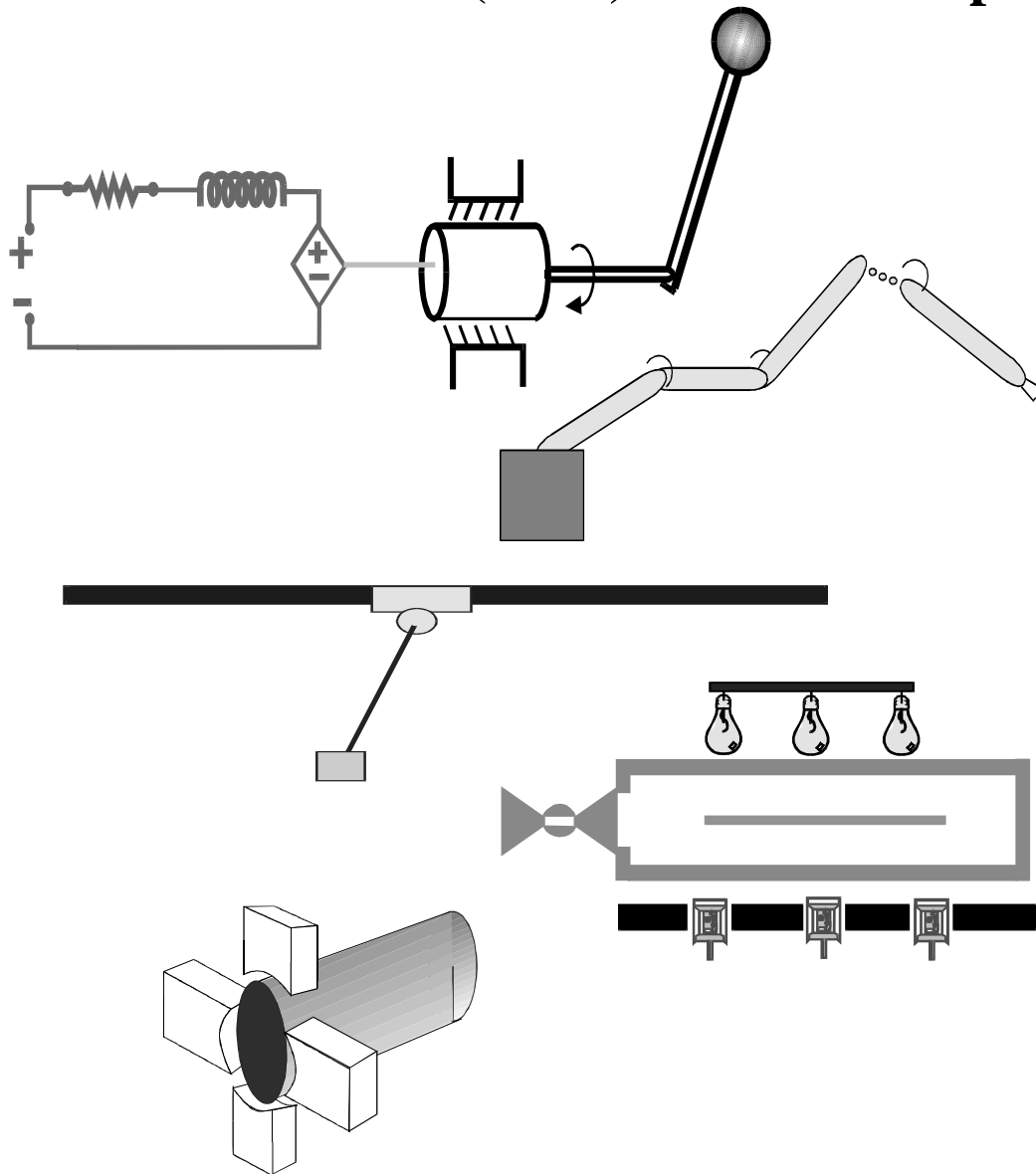# College of Engineering and Science
Control and Robotics (CRB) Technical Report

Number: CU/CRB/8/16/05/#1

Title: Passive Coordination of Nonlinear Bilateral Teleoperated Manipulators

Authors: M. McIntyre, W. Dixon, D. Dawson, and E. Tatlicioglu

Report Documentation Page		*Form Approved* *OMB No. 0704-0188*

Public reporting burden for the collection of information is estimated to average 1 hour per response, including the time for reviewing instructions, searching existing data sources, gathering and maintaining the data needed, and completing and reviewing the collection of information. Send comments regarding this burden estimate or any other aspect of this collection of information, including suggestions for reducing this burden, to Washington Headquarters Services, Directorate for Information Operations and Reports, 1215 Jefferson Davis Highway, Suite 1204, Arlington VA 22202-4302. Respondents should be aware that notwithstanding any other provision of law, no person shall be subject to a penalty for failing to comply with a collection of information if it does not display a currently valid OMB control number.

1. REPORT DATE **2005**	2. REPORT TYPE	3. DATES COVERED **00-00-2005 to 00-00-2005**

4. TITLE AND SUBTITLE **Passive Coordination of Nonlinear Bilateral Teleoperated Manipulators**	5a. CONTRACT NUMBER
	5b. GRANT NUMBER
	5c. PROGRAM ELEMENT NUMBER
6. AUTHOR(S)	5d. PROJECT NUMBER
	5e. TASK NUMBER
	5f. WORK UNIT NUMBER

7. PERFORMING ORGANIZATION NAME(S) AND ADDRESS(ES) **Clemson University,Department of Electrical & Computer Engineering,Clemson,SC,29634-0915**	8. PERFORMING ORGANIZATION REPORT NUMBER

9. SPONSORING/MONITORING AGENCY NAME(S) AND ADDRESS(ES)	10. SPONSOR/MONITOR'S ACRONYM(S)
	11. SPONSOR/MONITOR'S REPORT NUMBER(S)

12. DISTRIBUTION/AVAILABILITY STATEMENT
Approved for public release; distribution unlimited

13. SUPPLEMENTARY NOTES

14. ABSTRACT

15. SUBJECT TERMS

16. SECURITY CLASSIFICATION OF:			17. LIMITATION OF ABSTRACT	18. NUMBER OF PAGES **35**	19a. NAME OF RESPONSIBLE PERSON
a. REPORT **unclassified**	b. ABSTRACT **unclassified**	c. THIS PAGE **unclassified**			

Standard Form 298 (Rev. 8-98)
Prescribed by ANSI Std Z39-18

Passive Coordination of Nonlinear Bilateral Teleoperated Manipulators*

M. McIntyre,[†] W. Dixon,[‡] D. Dawson,[†]and E. Tatlicioglu[†]

[†]Department of Electrical & Computer Engineering, Clemson University, Clemson, SC 29634-0915

[‡]Department of Mechanical & Aerospace Engineering, University of Florida, Gainesville, FL 32611-6250

E-mail: mmcinty@clemson.edu, wdixon@ufl.edu, darren.dawson@ces.clemson.edu, etatlic@clemson.edu

Abstract: Significant research has been aimed at the development and control of teleoperator systems due to both the practical importance and the challenging theoretical nature of the problem. Two controllers are developed in this paper for a nonlinear teleoperator system that target coordination of the master and slave manipulators and passivity of the overall system. The first controller is proven to yield a semi-global asymptotic result in the presence of parametric uncertainty in the master and slave manipulator dynamic models. The second controller yields a global asymptotic result despite unmeasurable user and environmental input forces. To develop each controller, a transformation encodes the coordination and passivity objectives in the closed loop system. The coordinated system is forced to track a dynamic system to assist in meeting all control objectives. Finally, continuous nonlinear integral feedback terms are used to accommodate for incomplete system knowledge for both controllers. Lyapunov-based techniques are used to prove that all control objectives are met and that all signals are bounded.

1   Introduction

A teleoperator system consists of a user interacting with some type of input device (i.e., a master manipulator) with the intention of imparting a predictable response by an output system (i.e., a slave manipulator). Significant research has been aimed at the development and control of teleoperator systems due to both practical importance and the challenging theoretical nature of this human-robot interaction problem. Practical applications of teleoperation are motivated by the need for task execution in hazardous environments (e.g., contaminated facilities, space, underwater), the need for remote manipulation due to the characteristics of the object (e.g., size and mass of an object, hazardous nature of the object), or the need for precision beyond human capacity (e.g., robotic assisted medical procedures). The teleoperator problem is theoretically challenging due to issues that impact the user's ability to impart a desired motion and a desired force on the remote environment through the coupled master-slave system. Some difficult issues include the presence of uncertainty in the master and slave dynamics, the ability to accurately model or measure environmental and user inputs to the system, the ability to safely reflect desired forces back to the user while mitigating other forces, and the stability of the overall system (e.g., as stated in [14], a

stable teleoperator system may be destabilized when interacting with a stable environment due to coupling between the systems).

The emphasis of some previous related research is to achieve ideal transparency by exactly transferring the slave robot impedance to the user. Typically, approaches that aim for ideal transparency either require a priori knowledge of the environmental inputs to the slave manipulator, as in [4], or estimate the impedance of the slave manipulator as in [6]. Some exceptions include the teleoperator controllers aimed at low-frequency transparency developed in [11] and [23] that do not require knowledge of the impedance of the user or environment. However, the approaches in [4], [6], [11], and [23] are based on linear teleoperator systems with frequency-based control designs. A review of other frequency-based approaches applied to linear teleoperator systems are given in [1], [8], [9], [22], and [25]. In [7], an adaptive nonlinear control design is presented that achieves transparency in the sense of motion and force tracking.

Other research has emphasized the stability and safe operation of the teleoperator system through passivity concepts (e.g., [1]-[3], [12]-[14], and [17]-[19]). In [1], Anderson and Spong used passivity and scattering criterion to propose a bilateral control law for a linear time-invariant teleoperator system in any environment and in the presence of time delay. These results were then extended in [18] and [19], where wave-variables were used to define a new configuration for force-reflecting teleoperators. In [19], and more recently in [2] and [3], these methods where extended to solve the position tracking problem. In [14], a passivity-based approach was used to develop a controller that renders a linear teleoperator system as a passive rigid mechanical tool with desired kinematic and power scaling capabilities. The development in [14] was extended to nonlinear teleoperator systems in [12] and [13]. The controllers in [12] and [13] are dependent on knowledge of the dynamics of the master and slave manipulator and force measurements.

In comparison to the previous literature, two controllers are developed in this paper for nonlinear teleoperator systems that target coordination of the master and slave manipulators as well as passivity of the overall system. The first controller is proven to yield a semi-global asymptotic result in the presence of parametric uncertainty in the master and slave manipulator dynamic models provided the user and environmental input forces are measurable; henceforth, referred to as the MIF, (measurable input force) controller. The second controller yields a global asymptotic result despite unmeasurable user and environmental input forces (UMIF) provided the dynamic models of the respective manipulators are known. The novelty in developing each controller resided in the three following steps. The first utilizes a transformation which encodes both the coordination and passivity objectives within the closed loop system. Next, a dynamic trajectory generating system is designed which assists in achieving overall system passivity as well as keeping all signals bounded in the closed loop system. Finally, a continuous nonlinear integral feedback observer (see [20] and [24]) is exploited to compensate for the lack of system dynamics information or user and environmental force measurements. For each controller, Lyapunov-based techniques are used to prove that these three steps develop a stable passively coordinated teleoperator system.

The controllers developed in this work utilize the nonlinear dynamic model which offers a clear advantage over past results for linear teleoperator systems ([4], [6], [11], and [23]). The MIF controller developed in Section 3 compensates for unknown system parameters, which offers an improvement over past works that require exact model knowledge (i.e. [4] and [6]). The UMIF controller developed in Section 4 compensates for unavailable force measurement, which offers an improvement over works that requires force measurements (i.e. [12] and [13]). Numerical simulation results are presented for each controller in Sections 3.4 and 4.4, respectively.

2

2 System Model

The dynamic model for a $2n$-DOF nonlinear teleoperator consisting of a revolute n-DOF master and a revolute n-DOF slave revolute robot are described by the following expressions [12]

$$\gamma \left\{ M_1(q_1(t))\ddot{q}_1(t) + C_1(q_1(t), \dot{q}_1(t))\dot{q}_1(t) + B_1\dot{q}_1(t) = T_1(t) + F_1(t) \right\} \tag{1}$$

$$M_2(q_2(t))\ddot{q}_2(t) + C_2(q_2(t), \dot{q}_2(t))\dot{q}_2(t) + B_2\dot{q}_2(t) = T_2(t) + F_2(t). \tag{2}$$

In (1) and (2), $\gamma \in \mathbb{R}$ denotes a positive adjustable power scaling term, $q_i(t), \dot{q}_i(t), \ddot{q}_i(t) \in \mathbb{R}^n$ denote the link position, velocity, and acceleration, respectively, $\forall i = 1, 2$ where $i = 1$ denotes the master manipulator and $i = 2$ denotes the slave manipulator, $M_i(q_i) \in \mathbb{R}^{n \times n}$ represents the inertia effects, $C_i(q_i, \dot{q}_i) \in \mathbb{R}^{n \times n}$ represents centripetal-Coriolis effects, $B_i \in \mathbb{R}^{n \times n}$ represents the constant positive definite, diagonal dynamic frictional effects, $T_i(t) \in \mathbb{R}^n$ represents the torque input control vector, $F_1(t) \in \mathbb{R}^n$ represents the user input force, and $F_2(t) \in \mathbb{R}^n$ represents the input force from the environment. The subsequent development is based on the property that the master and slave inertia matrices are positive definite and symmetric in the sense that [15]

$$m_{1i} \|\xi\|^2 \leq \xi^T M_i(q_i)\xi \leq m_{2i} \|\xi\|^2 \tag{3}$$

$\forall \xi \in \mathbb{R}^n$ and $i = 1, 2$ where $m_{1i}, m_{2i} \in \mathbb{R}$ are positive constants, and $\|\cdot\|$ denotes the Euclidean norm. The subsequent development is also based on the assumption that $q_i(t), \dot{q}_i(t)$ are measurable, and that the inertia and centripetal-Coriolis matrices are second order differentiable.

3 MIF Control Development

For the MIF controller development, the subsequent analysis will prove a semi-global asymptotic result in the presence of parametric uncertainty in the master and slave manipulator dynamic models provided the user and environmental input forces are measurable. This development requires the assumption that $F_i(t), \dot{F}_i(t), \ddot{F}_i(t) \in L_\infty \; \forall i = 1, 2$ (precedence for this type of assumption is provided in [12] and [14]).

3.1 Objective and Model Transformation

One of the two primary objectives for the bilateral teleoperator system is to ensure coordination between the master and the slave manipulators in the following sense

$$q_2(t) \to q_1(t) \text{ as } t \to \infty. \tag{4}$$

The other primary objective is to ensure that the system remains passive with respect to the scaled user and environmental power in the following sense [12]

$$\int_{t_0}^{t} (\gamma \dot{q}_1^T(\tau)F_1(\tau) + \dot{q}_2^T(\tau)F_2(\tau))d\tau \geq -c_1^2 \tag{5}$$

where $c_1 \in \mathbb{R}$ is a bounded positive constant, and γ was introduced in (1). The passivity objective is included in this section to ensure that the human can interact with the robotic system in a stable and safe manner, and that the robot can also interact with the environment in a stable and safe manner. To facilitate the passivity objective in (5), an auxiliary control objective is utilized.

Specifically, the coordinated master and slave manipulators are forced to track a desired bounded trajectory, denoted by $q_d(t) \in \mathbb{R}^n$, in the sense that [13]

$$q_1(t) + q_2(t) \to q_d(t). \tag{6}$$

An additional objective is that all signals are required to remain bounded within the closed loop system.

To facilitate the subsequent development, a globally invertible transformation is defined that encodes both the coordination and passivity objectives as follows

$$x \triangleq Sq \tag{7}$$

where $x(t) \triangleq [x_1^T(t) \; x_2^T(t)]^T \in \mathbb{R}^{2n}$, $q(t) \triangleq [q_1^T(t) \; q_2^T(t)]^T \in \mathbb{R}^{2n}$, and $S \in \mathbb{R}^{2n \times 2n}$ is defined as follows

$$S \triangleq \begin{bmatrix} I & -I \\ I & I \end{bmatrix} \qquad S^{-1} = \frac{1}{2} \begin{bmatrix} I & I \\ -I & I \end{bmatrix} \tag{8}$$

where $I \in \mathbb{R}^{n \times n}$ denotes the identity matrix. Based on (7), the dynamic models given in (1) and (2) can be expressed as follows

$$\bar{M}(x)\ddot{x} + \bar{C}(x, \dot{x})\dot{x} + \bar{B}\dot{x} = \bar{T}(t) + \bar{F}(t) \tag{9}$$

where

$$\bar{M}(x) = S^{-T} \begin{bmatrix} \gamma M_1 & 0_{2n} \\ 0_{2n} & M_2 \end{bmatrix} S^{-1} \in \mathbb{R}^{2n \times 2n} \tag{10}$$

$$\bar{C}(x, \dot{x}) = S^{-T} \begin{bmatrix} \gamma C_1 & 0_{2n} \\ 0_{2n} & C_2 \end{bmatrix} S^{-1} \in \mathbb{R}^{2n \times 2n} \tag{11}$$

$$\bar{B} = S^{-T} \begin{bmatrix} \gamma B_1 & 0_{2n} \\ 0_{2n} & B_2 \end{bmatrix} S^{-1} \in \mathbb{R}^{2n \times 2n} \tag{12}$$

$$\bar{T}(t) = S^{-T} \begin{bmatrix} \gamma T_1^T & T_2^T \end{bmatrix}^T \in \mathbb{R}^{2n} \tag{13}$$

$$\bar{F}(t) \triangleq \begin{bmatrix} \bar{F}_1(t) \\ \bar{F}_2(t) \end{bmatrix} = S^{-T} \begin{bmatrix} \gamma F_1 \\ F_2 \end{bmatrix} \in \mathbb{R}^{2n} \tag{14}$$

and $0_{2n} \in \mathbb{R}^{n \times n}$ denotes an $n \times n$ matrix of zeros. The subsequent development is based on the property that $\bar{M}(x)$, as defined in (10), is a positive definite and symmetric matrix in the sense that [15]

$$\bar{m}_1 \|\xi\|^2 \le \xi^T \bar{M}(x)\xi \le \bar{m}_2 \|\xi\|^2 \tag{15}$$

$\forall \xi \in \mathbb{R}^{2n}$ where $\bar{m}_1$, $\bar{m}_2 \in \mathbb{R}$ are positive constants. It is also noted that $\bar{M}(x)$ is second order differentiable by assumption.

To facilitate the subsequent development and analysis, the control objectives can be combined through a filtered tracking error signal, denoted by $r(t) \in \mathbb{R}^{2n}$, that is defined as follows

$$r \triangleq \dot{e}_2 + \alpha_1 e_2 \tag{16}$$

where $e_2(t) \in \mathbb{R}^{2n}$ is defined as follows

$$e_2 \triangleq \dot{e}_1 + \alpha_2 e_1 \tag{17}$$

4

where α_1, $\alpha_2 \in \mathbb{R}$ are positive control gains, and $e_1(t) \in \mathbb{R}^{2n}$ is defined as follows

$$e_1 \triangleq x_d - x \tag{18}$$

where $x_d(t) \in \mathbb{R}^{2n}$ is defined as follows

$$x_d \triangleq \begin{bmatrix} 0_n^T & q_d^T(t) \end{bmatrix}^T \tag{19}$$

where $0_n \in \mathbb{R}^n$ denotes an $n \times 1$ vector of zeros. Based on the definition of $x(t)$ in (7) and $e_1(t)$ in (18), it is clear that if $\|e_1(t)\| \to 0$ as $t \to \infty$ then $q_2(t) \to q_1(t)$ and that $q_1(t) + q_2(t) \to q_d(t)$ as $t \to \infty$.

The desired trajectory $q_d(t)$ introduced in (6) and (19) is generated by the following expression

$$M_T \ddot{q}_d + B_T \dot{q}_d + K_T q_d = \bar{F}_2. \tag{20}$$

In (20), M_T, B_T, $K_T \in \mathbb{R}^{n \times n}$ represent constant positive definite, diagonal matrices, and $\bar{F}_2(t)$ was introduced in (14). Based on the assumption that $\bar{F}_2(t) \in \mathcal{L}_\infty$, standard linear analysis techniques can be used to prove that $q_d(t)$, $\dot{q}_d(t)$, $\ddot{q}_d(t) \in \mathcal{L}_\infty$. The time derivative of (20) is given by the following expression

$$M_T \dddot{q}_d + B_T \ddot{q}_d + K_T \dot{q}_d = \dot{\bar{F}}_2 . \tag{21}$$

From (21), the fact that $\dot{q}_d(t)$, $\ddot{q}_d(t) \in \mathcal{L}_\infty$, and the assumption that $\dot{\bar{F}}_2(t) \in \mathcal{L}_\infty$, it is clear that $\dddot{q}_d(t) \in \mathcal{L}_\infty$. By taking the time derivative of (21), and utilizing the assumption that $\ddot{\bar{F}}_2(t) \in \mathcal{L}_\infty$, we can also show that $\ddddot{q}_d(t) \in \mathcal{L}_\infty$.

3.2 Closed-Loop Error System

Based on the assumption that the user and environmental forces are measurable, the control input $\bar{T}(t)$ of (13) is designed as follows

$$\bar{T} \triangleq \bar{u} - \bar{F} \tag{22}$$

where $\bar{u}(t) \in \mathbb{R}^{2n}$ is an auxiliary control input. Substituting (22) into (9) yields the following simplified system

$$\bar{M}\ddot{x} + \bar{C}\dot{x} + \bar{B}\dot{x} = \bar{u}. \tag{23}$$

After taking the time derivative of (16) and premultiplying by $\bar{M}(x)$, the following expression can be obtained

$$\bar{M}\dot{r} = \bar{M}\dddot{x}_d + \dot{\bar{M}}\ddot{x} + \frac{d}{dt}\left[\bar{C}\dot{x} + \bar{B}\dot{x}\right] - \dot{\bar{u}} + \alpha_2 \bar{M}\ddot{e}_1 + \alpha_1 \bar{M}\dot{e}_2 \tag{24}$$

where (16)-(18), and the time derivative of (23) were utilized. To facilitate the subsequent analysis, the expression in (24) is rewritten as follows

$$\bar{M}\dot{r} = \tilde{N} + N_d - e_2 - \dot{\bar{u}} - \frac{1}{2}\dot{\bar{M}}r \tag{25}$$

5

where the auxiliary signal $\tilde{N}(x, \dot{x}, \ddot{x}, t) \in \mathbb{R}^{2n}$ is defined as

$$\tilde{N} \triangleq N - N_d \tag{26}$$

where $N(x, \dot{x}, \ddot{x}, t) \in \mathbb{R}^{2n}$ is defined as

$$N \triangleq \bar{M}\,\dddot{x}_d + \dot{\bar{M}}\,\ddot{x} + \alpha_2 \bar{M}\ddot{e}_1 + \alpha_1 \bar{M}\dot{e}_2 + e_2 + \frac{d}{dt}\left[\bar{C}\dot{x} + \bar{B}\dot{x}\right] + \frac{1}{2}\,\dot{\bar{M}}\,r \tag{27}$$

and $N_d(t) \in \mathbb{R}^{2n}$ is defined as

$$
\begin{aligned}
N_d &\triangleq N|_{x=x_d,\ \dot{x}=\dot{x}_d,\ \ddot{x}=\ddot{x}_d} \\
&= \bar{M}(x_d)\,\dddot{x}_d + \dot{\bar{M}}\,(x_d, \dot{x}_d)\ddot{x}_d + \frac{d}{dt}\left[\bar{C}(x_d, \dot{x}_d)\dot{x}_d + \bar{B}\dot{x}_d\right].
\end{aligned}
\tag{28}
$$

Remark 1 *To facilitate the subsequent analysis, the following upper bound can be developed for $\tilde{N}(\cdot)$*

$$\left\|\tilde{N}\right\| \le \rho\left(\|z\|\right)\|z\| \quad where \quad z \triangleq \begin{bmatrix} e_1^T & e_2^T & r^T \end{bmatrix}^T$$

and the positive function $\rho\left(\|z\|\right)$ is non-decreasing in $\|z\|$ (see Appendix F for further details).

Based on (25), the auxiliary control input $\bar{u}(t)$ introduced in (22) is designed as follows

$$\bar{u} \triangleq (k_s + 1)\left[e_2(t) - e_2(t_0) + \alpha_1 \int_{t_0}^{t} e_2(\tau)d\tau\right] + (\beta_1 + \beta_2)\int_{t_0}^{t} sgn(e_2(\tau))d\tau \tag{29}$$

where $k_s, \beta_1, \beta_2 \in \mathbb{R}$ are positive control gains, and $sgn(\cdot)$ denotes the vector signum function. The term $e_2(t_0)$ in (29) is included so that $\bar{u}(t_0) = 0$. The time derivative of (29) is given by the following expression

$$\dot{\bar{u}} = (k_s + 1)r + (\beta_1 + \beta_2)\,sgn(e_2). \tag{30}$$

Substituting (30) into (25) yields the following closed-loop error system

$$\bar{M}\dot{r} = -(k_s + 1)r - (\beta_1 + \beta_2)\,sgn(e_2) + \tilde{N} + N_d - e_2 - \frac{1}{2}\,\dot{\bar{M}}\,r. \tag{31}$$

Remark 2 *Based on the expressions in (19), (28) and the fact that $q_d(t)$, $\dot{q}_d(t)$, $\ddot{q}_d(t)$, $\dddot{q}_d(t)$, and $\ddddot{q}_d(t) \in \mathcal{L}_\infty$, then $\|N_d(t)\|$ and $\left\|\dot{N}_d(t)\right\|$ can be upper bounded by known positive constants $\varsigma_1, \varsigma_2 \in \mathbb{R}$ as follows*

$$\|N_d(t)\| \le \varsigma_1 \qquad \left\|\dot{N}_d(t)\right\| \le \varsigma_2. \tag{32}$$

3.3 Stability Analysis

Theorem 1 *The controller given in (22) and (29), ensures that all closed-loop signals are bounded and that coordination between the master and slave manipulators is achieved in the sense that*

$$q_2(t) \to q_1(t) \quad as \quad t \to \infty \tag{33}$$

provided the control gain β_1 introduced in (29) is selected to satisfy the following sufficient condition

$$\beta_1 > \varsigma_1 + \frac{1}{\alpha_1}\varsigma_2 \tag{34}$$

where ς_1 and ς_2 are given in (32), the control gains α_1 and α_2 are selected greater than 2, and k_s is selected sufficiently large with respect to the initial conditions of the system.

Proof. See Appendix A.

Theorem 2 *The controller given in (22) and (29) ensures that the teleoperator system is passive with respect to the scaled user and environmental power.*

Proof. See Appendix B.

3.4 Simulation Results

A numerical simulation was performed to demonstrate the performance of the controller given in (22) and (29). The following 2-link, revolute robot dynamic model was utilized for both the master and slave manipulators [21]

$$
\begin{bmatrix} \tau_{i_1} \\ \tau_{i_2} \end{bmatrix} + \begin{bmatrix} F_{i_1} \\ F_{i_2} \end{bmatrix} = \begin{bmatrix} p_{1_i} + 2p_{3_i}c(q_{i_2}) + 2p_{4_i}s(q_{i_2}) & p_{2_i} + p_{3_i}c(q_{i_2}) + p_{4_i}s(q_{i_2}) \\ p_{2_i} + p_{3_i}c(q_{i_2}) + p_{4_i}s(q_{i_2}) & p_{2_i} \end{bmatrix} \begin{bmatrix} \ddot{q}_{i_1} \\ \ddot{q}_{i_2} \end{bmatrix}
$$
$$
+ \begin{bmatrix} -(p_{3_i}s(q_{i_2}) - p_{4_i}c(q_{i_2}))\,\dot{q}_{i_2} & -(p_{3_i}s(q_{i_2}) - p_{4_i}c(q_{i_2}))\,(\dot{q}_{i_1} + \dot{q}_{i_2}) \\ (p_{3_i}s(q_{i_2}) - p_{4_i}c(q_{i_2}))\,\dot{q}_{i_1} & 0 \end{bmatrix} \begin{bmatrix} \dot{q}_{i_1} \\ \dot{q}_{i_2} \end{bmatrix}
$$
$$
+ \begin{bmatrix} f_{d1_i} & 0 \\ 0 & f_{d2_i} \end{bmatrix} \begin{bmatrix} \dot{q}_{i_1} \\ \dot{q}_{i_2} \end{bmatrix} \tag{35}
$$

where $s(\cdot)$ and $c(\cdot)$ denote the $sin(\cdot)$ and $cos(\cdot)$ functions. For the master manipulator, $i = 1$ and $p_{1_1} = 3.34$ [kg·m²], $p_{2_1} = 0.97$ [kg·m²], $p_{3_1} = 1.0392$ [kg·m²], $p_{4_1} = 0.6$ [kg·m²], $f_{d1_1} = 1.3$ [Nm·sec], and $f_{d2_1} = 0.88$ [Nm·sec]. For the slave manipulator, $i = 2$ and $p_{1_2} = 2.67$ [kg·m²], $p_{2_2} = 1.455$ [kg·m²], $p_{3_2} = 0.929$ [kg·m²], $p_{4_2} = 0.537$ [kg·m²], $f_{d1_2} = 1.3$ [Nm·sec], and $f_{d2_2} = 0.88$ [Nm·sec], where the parameters are based on [21]. For this simulation, the positive adjustable power scaling term was selected as $\gamma = 1$. The user input force vector was set equal to the following arbitrary periodic time-varying signals

$$
\begin{bmatrix} F_{1_1} \\ F_{1_2} \end{bmatrix} = \begin{bmatrix} 25\sin(1.1t) \\ 35\sin(t) \end{bmatrix}. \tag{36}
$$

To emulate contact with the environment, a spring-like input force vector was selected as follows

$$
\begin{bmatrix} F_{2_1} \\ F_{2_2} \end{bmatrix} = \begin{bmatrix} -0.6\dot{q}_{1_2} - q_{1_2} \\ -0.6\dot{q}_{2_2} - q_{2_2} \end{bmatrix}. \tag{37}
$$

To assist in meeting the passivity control objective, the coordinated teleoperated system must follow a desired trajectory which was generated by the system described by (20) and for this simulation was selected as follows

$$
\bar{F}_2(t) = \begin{bmatrix} 5 & 0 \\ 0 & 5 \end{bmatrix} \begin{bmatrix} \ddot{q}_{d1} \\ \ddot{q}_{d2} \end{bmatrix} + \begin{bmatrix} 3 & 0 \\ 0 & 3 \end{bmatrix} \begin{bmatrix} \dot{q}_{d1} \\ \dot{q}_{d2} \end{bmatrix} + \begin{bmatrix} 1 & 0 \\ 0 & 1 \end{bmatrix} \begin{bmatrix} q_{d1} \\ q_{d2} \end{bmatrix} \tag{38}
$$

where $q_{d1}(t)$ and $q_{d2}(t)$ denote the desired link positions, and $\bar{F}_2(t)$ is equal to the following expression

$$
\bar{F}_2(t) = \frac{1}{2}\left(\gamma F_1(t) + F_2(t)\right)
$$

where $\bar{F}_2(t)$ was defined in (14).

7

The actual trajectory for the master and slave manipulators are demonstrated in Figure 1 for controller gains selected as $k_s = 100$ and $\beta_1 + \beta_2 = 25$. The link position tracking error between the master and slave manipulators can be seen in Figure 2. From Figures 1 and 2, it is clear that the coordination control objective is achieved. The actual trajectory for the coordinated system $(q_1(t) + q_2(t))$ and the desired trajectory as defined by (38), are demonstrated in Figure 3. The coordinated system versus the desired trajectory tracking error as defined by $q_1(t) + q_2(t) - q_d(t)$, is given in Figure 4. From Figures 3 and 4, it is clear that the coordinated system tracks the desired trajectory. The control torque inputs for the master and slave manipulator are provided in Figures 5 and 6, respectively.
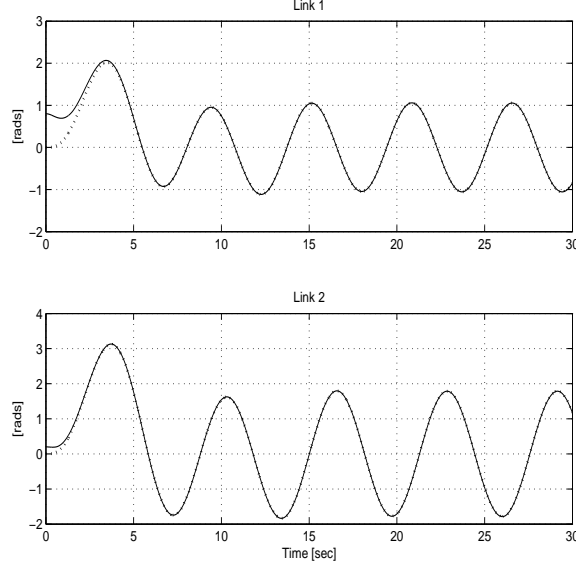

Figure 1: Actual trajectory for master (i.e., $q_1(t)$) (—) and slave (i.e., $q_2(t)$) (- -) manipulators for Link 1 and Link 2.

4 UMIF Control Development

For the UMIF controller development, the subsequent analysis will prove a global asymptotic result despite unmeasurable user and environmental input forces (UMIF) provided the dynamic models of the respective manipulators are known. This development also requires the assumption that $F_i(t)$, $\dot{F}_i(t)$, $\ddot{F}_i(t) \in L_\infty \ \forall i = 1, 2$.

4.1 Objective and Model Transformation

One of the two primary objectives for the bilateral teleoperator system is to ensure coordination between the master and the slave manipulators as in (4). The other objective is to ensure that the system remains passive with respect to the scaled user and environmental power as in (5). To assist in meeting the passivity objective the following desired trajectory, defined as $x_d(t) \in \mathbb{R}^{2n}$, is generated by the following dynamic system

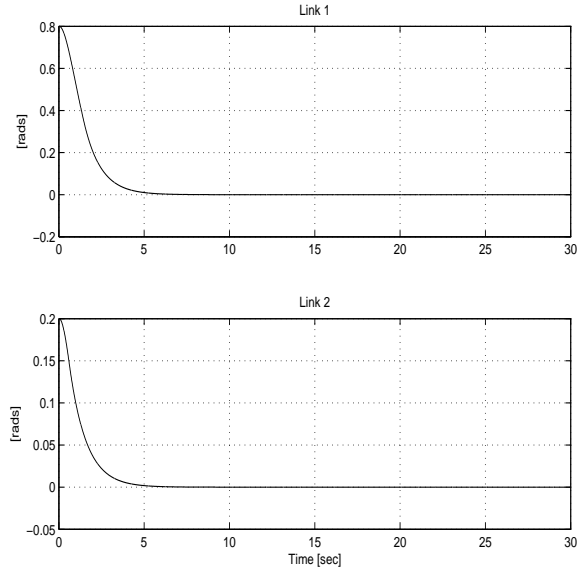$$\bar{M}\ddot{x}_d + B_T\dot{x}_d + K_T x_d + \frac{1}{2}\dot{\bar{M}}\dot{x}_d = \hat{F}. \tag{39}$$

8

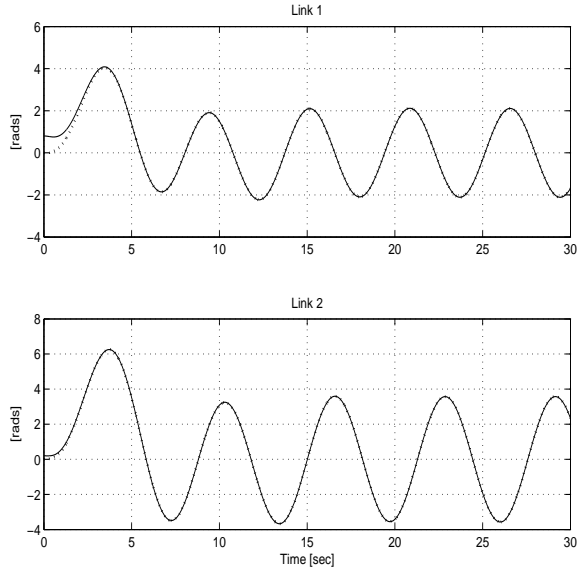Figure 2: Link position tracking error between the master and slave manipulators (i.e., $q_1(t) - q_2(t)$).

Figure 3: Actual coordinated (i.e., $q_1(t) + q_2(t)$) trajectory (—) and desired (i.e., $q_d(t)$) trajectory (- -) for Link 1 and Link 2.
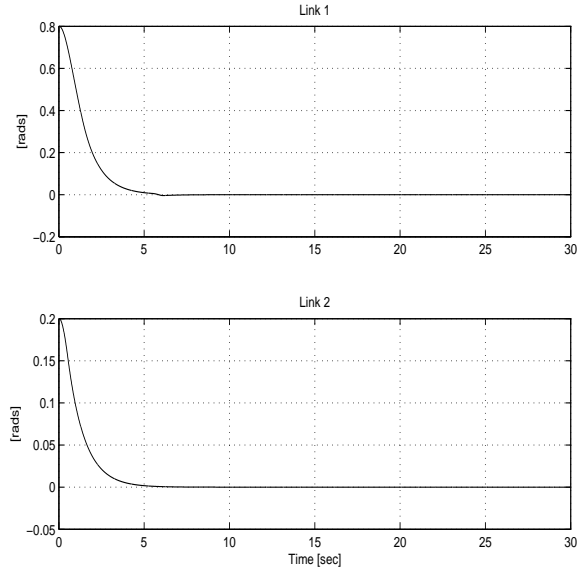
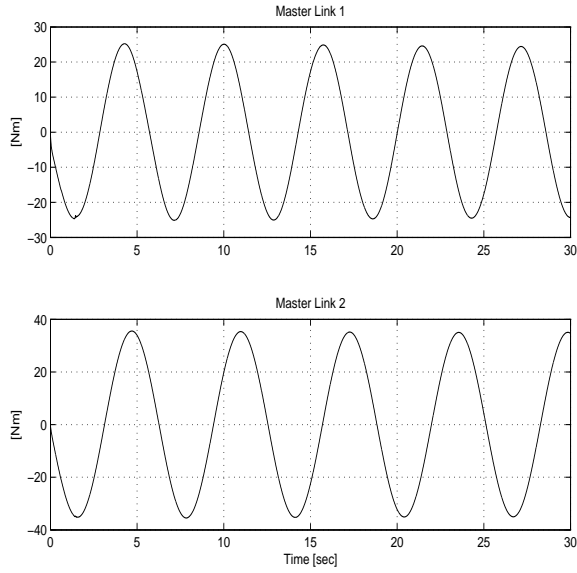Figure 4: The coordinated system versus the desired trajectory tracking error (i.e., $q_1(t) + q_2(t) - q_d(t)$).

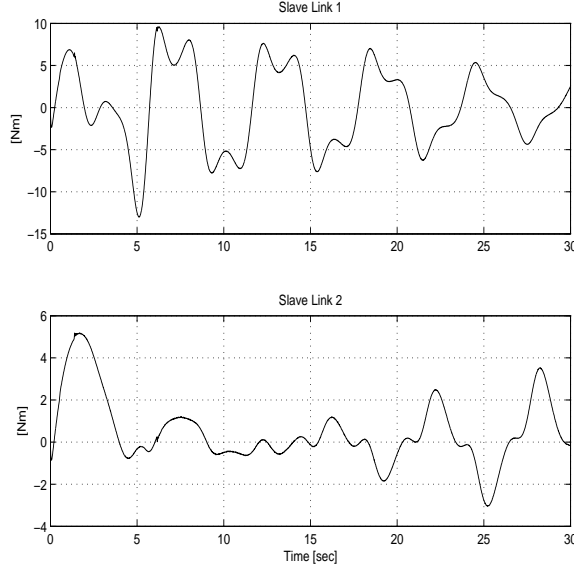Figure 5: Master manipulator control input torque (i.e., $\tau_1(t)$).

10

Figure 6: Slave manipulator control input torque (i.e., $\tau_2(t)$).

In (39), $\bar{M}(x)$ was defined in (10), B_T and $K_T \in \mathbb{R}^{2n \times 2n}$ represent constant positive definite, diagonal matrices, and $\hat{F}(t) \in \mathbb{R}^{2n}$ is a subsequently designed nonlinear force observer, and $x_d(t) \in \mathbb{R}^{2n}$ can be decomposed as follows

$$x_d = \begin{bmatrix} x_{d1}^T(t) & x_{d2}^T(t) \end{bmatrix}^T \tag{40}$$

where $x_{d1}(t)$, $x_{d2}(t) \in \mathbb{R}^n$. Subsequent development will prove that $\hat{F}(t) \in \mathcal{L}_\infty$. Based on this fact, the development in Appendix C can be used to prove that $x_d(t)$, $\dot{x}_d(t) \in \mathcal{L}_\infty$, then (39) can be used to prove that $\ddot{x}_d(t) \in \mathcal{L}_\infty$ as shown later, the passivity objective is facilitated by ensuring that the coordinated master and slave manipulators are forced to track a desired bounded trajectory $x_{d2}(t)$ in the sense that

$$q_1(t) + q_2(t) \rightarrow x_{d2}(t) \tag{41}$$

where $x_{d2}(t)$ was defined in (40). An additional objective is that all signals are required to remain bounded within the closed loop system.

To facilitate the subsequent development, a globally invertible transformation is defined that encodes both the coordination and passivity objectives as follows

$$x \triangleq Sq + \begin{bmatrix} x_{d1} \\ 0_n \end{bmatrix} \tag{42}$$

where $x(t) \triangleq [x_1^T(t) \ x_2^T(t)]^T \in \mathbb{R}^{2n}$, $q(t) \triangleq [q_1^T(t) \ q_2^T(t)]^T \in \mathbb{R}^{2n}$, $x_{d1}(t) \in \mathbb{R}^n$ was defined in (40), the zero vector $0_n \in \mathbb{R}^n$ and $S \in \mathbb{R}^{2n \times 2n}$ was defined in (8). Based on (42), the dynamic models given in (1) and (2) can be expressed as follows

$$\bar{M}(x)\ddot{x} - \bar{M}(x)\begin{bmatrix} \ddot{x}_{d1} \\ 0_n \end{bmatrix} + \bar{C}(x,\dot{x})\dot{x} - \bar{C}(x,\dot{x})\begin{bmatrix} \dot{x}_{d1} \\ 0_n \end{bmatrix} + \bar{B}\dot{x} - \bar{B}\begin{bmatrix} \dot{x}_{d1} \\ 0_n \end{bmatrix} = \bar{T}(t) + \bar{F}(t) \tag{43}$$

where $\bar{M}(x)$, $\bar{C}(x,\dot{x})$, $\bar{B}$, $\bar{T}(t)$, and $\bar{F}(t)$ were defined in (10)-(14).

11

To facilitate the subsequent UMIF development and analysis, the control objectives can be combined through a filtered tracking error signal denoted by $r(t) \in \mathbb{R}^{2n}$, that is defined as follows

$$r \triangleq \dot{e}_2 + e_2 \tag{44}$$

where $e_2(t) \in \mathbb{R}^{2n}$ is now defined as follows

$$e_2 \triangleq \bar{M} \left(\dot{e}_1 + \alpha_2 e_1 \right) \tag{45}$$

where $\alpha_2 \in \mathbb{R}$ is a positive control gain, and $e_1(t) \in \mathbb{R}^{2n}$ was defined in (18) as follows

$$e_1 \triangleq x_d - x$$

where $x_d(t)$ was defined in (40).

4.2 Closed Loop Error System

To facilitate the development of the closed-loop error system for $r(t)$, we first examine the error system dynamics for $e_1(t)$ and $e_2(t)$. To this end, we take the second time derivative of $e_1(t)$ and premultiply by $\bar{M}(x)$ to obtain the following expression

$$
\begin{aligned}
\bar{M}\ddot{e}_1 \;=\; & \hat{F} - B_T \dot{x}_d - K_T x_d - \frac{1}{2}\dot{\bar{M}}\,\dot{x}_d - \bar{T} - \bar{F} \\
& -\bar{M}\begin{bmatrix} \ddot{x}_{d1} \\ 0_n \end{bmatrix} + \bar{C}\dot{x} - \bar{C}\begin{bmatrix} \dot{x}_{d1} \\ 0_n \end{bmatrix} + \bar{B}\dot{x} - \bar{B}\begin{bmatrix} \dot{x}_{d1} \\ 0_n \end{bmatrix}
\end{aligned}
\tag{46}
$$

where (43) and (39) were utilized. Based on the assumption of exact model knowledge, the control input $\bar{T}(t)$ is designed as follows

$$
\begin{aligned}
\bar{T} \;\triangleq\; & \bar{T}_1 - B_T \dot{x}_d - K_T x_d - \frac{1}{2}\dot{\bar{M}}\,\dot{x}_d \\
& -\bar{M}\begin{bmatrix} \ddot{x}_{d1} \\ 0_n \end{bmatrix} + \bar{C}\dot{x} - \bar{C}\begin{bmatrix} \dot{x}_{d1} \\ 0_n \end{bmatrix} + \bar{B}\dot{x} - \bar{B}\begin{bmatrix} \dot{x}_{d1} \\ 0_n \end{bmatrix}
\end{aligned}
\tag{47}
$$

where $\bar{T}_1(t) \in \mathbb{R}^{2n}$ is an auxiliary control input. Substituting (47) into (46) yields the following simplified expression

$$\bar{M}\ddot{e}_1 = \hat{F} - \bar{F} - \bar{T}_1. \tag{48}$$

Based on (48), the time derivative of $e_2(t)$ in (45) can be obtained as follows

$$\dot{e}_2 = \dot{\bar{M}}\,\dot{e}_1 + \alpha_2 \dot{\bar{M}}\,e_1 + \alpha_2 \bar{M}\dot{e}_1 + \hat{F} - \bar{F} - \bar{T}_1. \tag{49}$$

Based on the expression in (49), the auxiliary control input $\bar{T}_1(t)$ is designed as follows

$$\bar{T}_1 \triangleq \dot{\bar{M}}\,\dot{e}_1 + \alpha_2 \dot{\bar{M}}\,e_1 + \alpha_2 \bar{M}\dot{e}_1. \tag{50}$$

After substituting (50) into (49), the following can be written

$$\dot{e}_2 = \hat{F} - \bar{F}. \tag{51}$$

Taking the time derivative of (51) yields the resulting expression

$$\ddot{e}_2 = \dot{\hat{F}} - \dot{F} . \tag{52}$$

The following error system dynamics can now be obtained for $r(t)$ by taking the time derivative of (44)

$$\dot{r} = r - e_2 + \dot{\hat{F}} - \dot{F} \tag{53}$$

where (44) and (52) were both utilized. Based on (53) and the subsequent stability analysis, the proportional-integral like nonlinear force observer $\hat{F}(t)$ introduced in (39) is designed as follows

$$\hat{F} \triangleq -(k_s + 1)\left[e_2(t) - e_2(t_0) + \int_{t_0}^t e_2(\tau)d\tau\right] - (\beta_1 + \beta_2)\int_{t_0}^t sgn\left(e_2(\tau)\right) d\tau \tag{54}$$

where k_s, β_1, and $\beta_2 \in \mathbb{R}$ are positive control gains, and $sgn(\cdot)$ denotes the vector signum function. The expression given in (54) is designed such that $\hat{F}(t_0) = 0$. The time derivative of (54) is given by the following expression

$$\dot{\hat{F}} = -(k_s + 1)r - (\beta_1 + \beta_2) sgn\left(e_2\right). \tag{55}$$

Substituting (55) into (53) yields the following closed loop error system

$$\dot{r} = -e_2 - \dot{F} - k_s r - (\beta_1 + \beta_2) sgn\left(e_2\right). \tag{56}$$

Remark 3 *Based on (14) and the assumption that $F_i(t)$, $\dot{F}_i(t)$, $\ddot{F}_i(t) \in L_\infty$ $\forall i = 1, 2$, upper bounds can be developed for $\left\|\dot{F}(t)\right\|$ and $\left\|\ddot{F}(t)\right\|$ as follows*

$$\left\|\dot{F}(t)\right\| \leq \varsigma_3 \qquad \left\|\ddot{F}(t)\right\| \leq \varsigma_4 \tag{57}$$

where $\varsigma_3, \varsigma_4 \in \mathbb{R}$ denote positive constants.

4.3 Stability Analysis

Theorem 3 *The controller given in (47) and (50) ensures that all closed-loop signals are bounded and that coordination between the master and slave manipulators is achieved in the sense that*

$$q_2(t) \to q_1(t) \quad as \quad t \to \infty \tag{58}$$

provided the control gain β_1, introduced in (54) is selected to satisfy the sufficient condition

$$\beta_1 > \varsigma_3 + \varsigma_4, \tag{59}$$

where ς_3 and ς_4 were introduced in (57).

Proof. See Appendix D.

Theorem 4 *The controller given in (47) and (50), ensures that the teleoperator system is passive with respect to the scaled user and environmental power.*

Proof. See Appendix E.

13

4.4 Simulation Results

A numerical simulation was performed for the controller given in (47) and (50). The 2-link, revolute robot dynamic model utilized in (35) was utilized for both the master and slave manipulators. The user input force vector in (36) and the environmental input force vector in (37) were also utilized.

To meet the passivity-based control objective, the coordinated teleoperated system must follow a desired trajectory, which is generated from (39) using the same parameter values for the transformed inertia matrix. The values for B_T, $K_T \in \mathbb{R}^{4 \times 4}$ were set to the following values

$$
\begin{aligned}
B_T &= diag\{5, 5, 5, 5\} \\
K_T &= diag\{25, 25, 25, 25\}
\end{aligned}
$$

where B_T and K_T are both diagonal matrices.

The actual trajectory for the master and slave manipulators are demonstrated in Figure 7 where the control gains were selected as $k_s = 100$, $\beta_1 + \beta_2 = 100$, and $\alpha_2 = 200$. The link position tracking error between the master and slave manipulators can be seen in Figure 8. From Figures 7 and 8, it is clear that the coordination control objective is achieved. The actual trajectory for the coordinated system $(q_1(t) + q_2(t))$ and the desired trajectory as defined in (39), are demonstrated in Figure 9. The coordinated system versus the desired trajectory tracking error as defined by $q_1(t) + q_2(t) - x_{d2}(t)$, is given in Figure 10. From Figures 9 and 10, it is clear that the coordinated system tracks the desired trajectory. The output of the nonlinear force observer is provided in Figure 11. The control torque inputs for both the master and slave manipulators are provided in Figures 12 and 13, respectively.
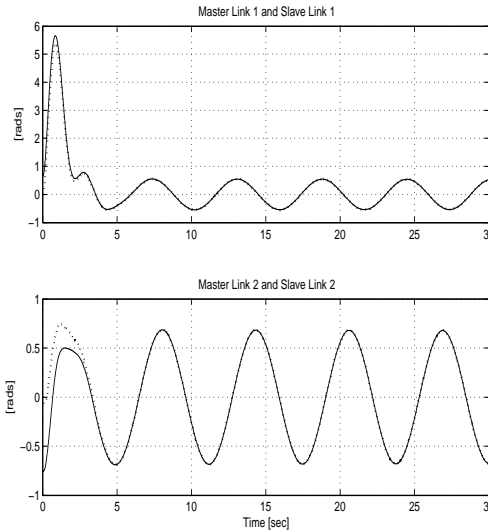

Figure 7: Actual trajectory for master (i.e., $q_1(t)$) (—) and slave (i.e., $q_2(t)$) (- -) manipulators for Link 1 and Link 2.

5 Conclusions

Through the use of transformations, dynamic trajectory generations, and continuous nonlinear integral feedback terms, two controllers were proven through Lyapunov-based techniques to passively
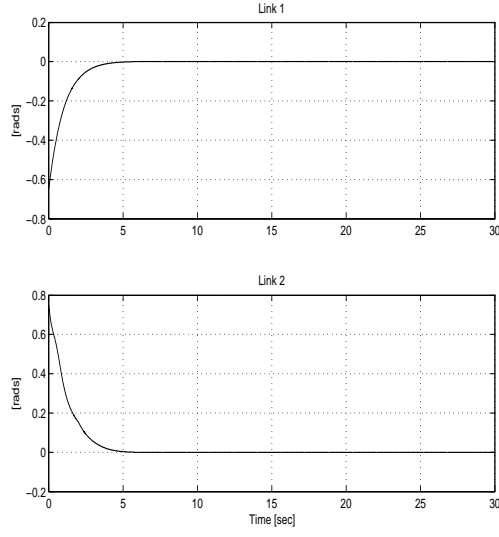
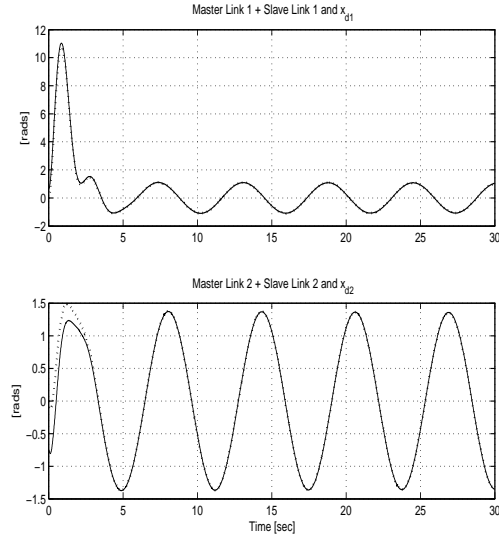Figure 8: Link position tracking error between the master and slave manipulators (i.e., $q_1(t) - q_2(t)$).

Figure 9: Actual coordinated (i.e., $q_1(t) + q_2(t)$) trajectory (—) and desired (i.e., $q_d(t)$) trajectory (- -) for Link 1 and Link 2.
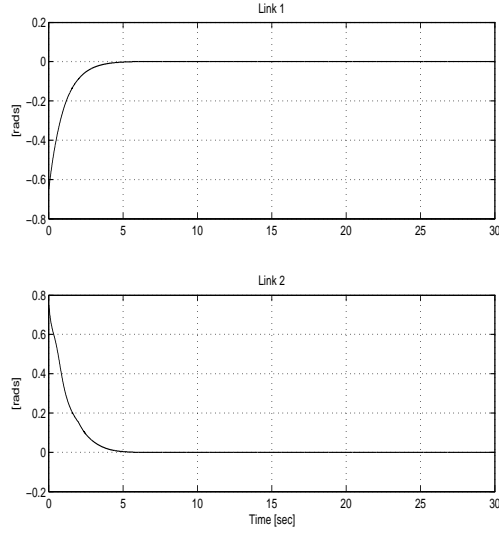
Figure 10: The coordinated system versus the desired trajectory tracking error (i.e., $q_1(t) + q_2(t) - x_{d2}(t)$).
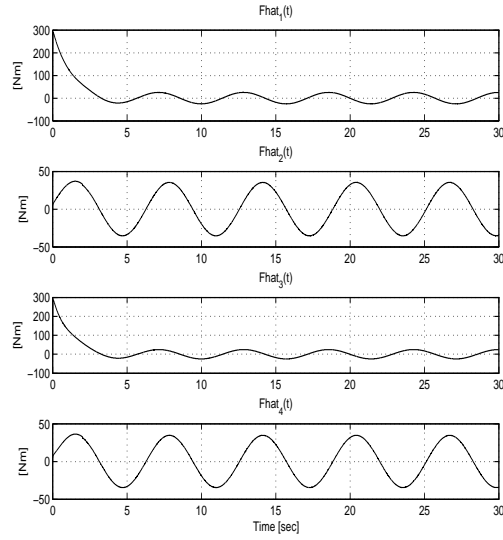

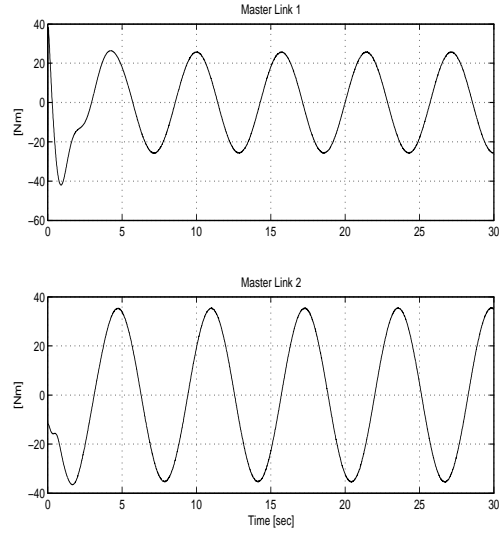Figure 11: The output of the nonlinear force observer (i.e. $\hat{F}(t)$) .

16

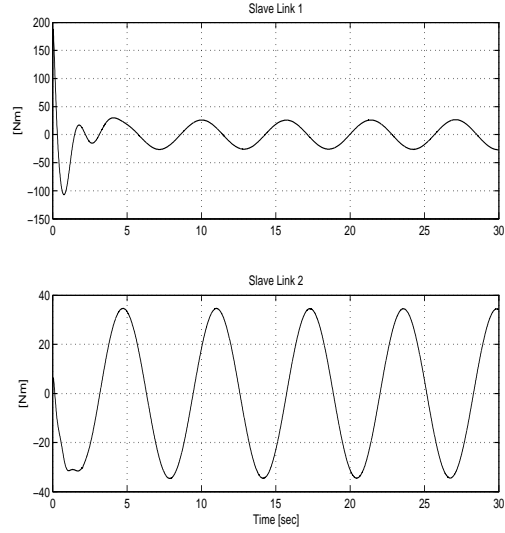Figure 12: Master manipulator control input torque (i.e., $\tau_1(t)$).

Figure 13: Slave manipulator control input torque (i.e., $\tau_2(t)$).

17

coordinate the master and slave manipulators with respect to the scaled user and environmental power despite incomplete system knowledge. Implementing either controller would provide the user of the closed loop teleoperator system with a power scalable, coordinated master-slave tool that provides safe and stable user feedback. The MIF controller was developed despite uncertainty in the dynamics of the teleoperator system resulting in a semi-global asymptotic result, and the UMIF controller was developed despite unmeasurable user and environmental force inputs resulting in a global asymptotic result. Simulation results demonstrate for both controllers that the coordination and tracking control objectives are met.

References

[1] R. J. Anderson and M. W. Spong, "Bilateral Control of Teleoperators with Time Delay," *IEEE Trans. on Automatic Control*, Vol. 34, No 5, pp. 494-501 (1989).

[2] N. Chopra, M. W. Spong, S. Hirche, and M. Buss, "Bilateral Teleoperation over the Internet: the Time Varying Delay Problem," *Proc. IEEE American Control Conference,* June 4-6, Denver, CO, 2003, pp. 155-160.

[3] N. Chopra, M. W. Spong, R. Ortega, and N. E. Barabanov, "On Position Tracking in Bilateral Teleoperators," *Proc. IEEE American Control Conference,* June 30-July 2, Boston, MA, 2004, pp. 5244-5249.

[4] J. E. Colgate, "Robust Impedance Shaping Telemanipulation," *IEEE Trans. on Robotics and Automation*, Vol. 9, No. 4, pp. 374-384 (1993).

[5] M. J. Corless and G. Leitmann, "Continuous State Feedback Guaranteeing Uniform Ultimate Boundedness for Uncertain Dynamic Systems," *IEEE Trans. on Automatic Control,* Vol. 26, No. 5, pp. 1139-1143 (1981).

[6] B. Hannaford, "A Design Framework for Teleoperators with Kinesthetic Feedback," *IEEE Trans. on Robotics and Automation*, Vol. 5, No. 4, pp. 426-434 (1989).

[7] N. V. Q. Hung, T. Narikiyo, H. D. Tuan, "Nonlinear Adaptive Control of Master-Slave System in Teleoperation," *Control Engineering Practice*, Vol. 11, No. 1, pp. 1-10 (2003).

[8] H. Kazerooni and C. L. Moore, "An Approach to Telerobotic Manipulations," *ASME J. Dynam. Syst., Meas., Contr.,* Vol. 119, No. 3, pp. 431-438 (1997).

[9] H. Kazerooni, T. I. Tsay, and K. Hollerbach, "A Controller Design Framework for Telerobotic Systems," *IEEE Trans. on Control Systems Technology,* Vol. 1, No. 1, pp. 50-62 (1993).

[10] H. Khalil, *Nonlinear Systems*, Third Edition, Prentice Hall: New Jersey, 1996.

[11] D. A. Lawrence, "Stability and Transparency in Bilateral Teleoperation," *IEEE Trans. on Robotics and Automation*, Vol. 9, No. 5, pp.624-637 (1993).

[12] D. Lee and P. Y. Li, "Passive Coordination Control of Nonlinear Bilateral Teleoperated Manipulators," *Proc. IEEE Int. Conf. Robotics and Automation,* May 11-15, Washington, DC, 2002, pp. 3278-3283.

[13] D. Lee and P. Y. Li, "Passive tool dynamics rendering for nonlinear bilateral teleoperated manipulators," *Proc. IEEE Int. Conf. Robotics and Automation,* May 11-15, Washington, DC, 2002, pp. 3284-3289.

[14] D. Lee and P. Y. Li, "Passive Bilateral Feedforward Control of Linear Dynamically Similar Teleoperated Manipulators," *IEEE Trans. on Robotics and Automation,* Vol. 19, No. 3, pp. 443-456 (2003).

[15] F. L. Lewis, D. M. Dawson, and C. T. Abdallah, Robot Manipulator Control: Theory and Practice, New York, NY: Marcel Dekker, Inc., 2004.

[16] M. McIntyre, W. Dixon, D. Dawson, and E. Tatlicioglu, "Passive Coordination of Nonlinear Bilateral Teleoperated Manipulators," Clemson University CRB Technical Report, CU/CRB/8/16/05/#1, http://www.ces.clemson.edu/ece/crb/publictn/tr.htm.

[17] B. E. Miller, J. E. Colgate, and R. A. Freeman, "Guaranteed Stability of Haptic Systems with Nonlinear Virtual Environments," *IEEE Trans. on Robotics and Automation,* Vol. 16, No. 6, pp. 712-719 (2000).

[18] G. Niemeyer, and J. J. E. Slotine, "Stable Adaptive Teleoperation," *IEEE Journal of Oceanic Engineering,* Vol. 16, No. 1, pp. 152-162 (1991).

[19] G. Niemeyer, and J. J. E. Slotine, "Designing Force Reflecting Teleoperators with Large Time Delays to Appear as Virtual Tools," *Proc. IEEE Int. Conf. Robotics and Automation,* April 20-25, Albuquerque, NM, 1997, pp. 2212-2218.

[20] Z. Qu and J. -X. Xu, "Model-Based Learning Controls and Their Comparisons Using Lyapunov Direct Method," *Asian Journal of Control,* Vol. 4, No. 1, pp. 99-110 (2002).

[21] J. J. E. Slotine and W. Li, Applied Nonlinear Control, Englewood Cliff, NJ: Prentice Hall, Inc., 1991.

[22] S. E. Salcudean, N. M. Wong, and R. L. Hollis, "Design and Control of a Force-Reflecting Teleoperation System with Magnetically Levitated Master and Wrist," *IEEE Trans. on Robotics and Automation,* Vol. 11, No. 6, pp. 844-858 (1995).

[23] S. E. Salcudean, M. Zhu, W. -H. Zhu, and K. Hashtudi-Zaad, "Transparent Bilateral Teleoperation Under Position and Rate Control," *Int. J. Robot. Res.,* Vol. 19, No. 12, pp. 1185-1202 (2000).

[24] B. Xian, M. S. de Queiroz, and D. M. Dawson, "A Continuous Control Mechanism for Uncertain Nonlinear Systems," *Optimal Control, Stabilization, and Nonsmooth Analysis, Lecture Notes in Control and Information Sciences,* Heidelberg, Germany: Springer-Verlag, pp. 251-262, 2004.

[25] Y. Yokokohji and T. Yoshikawa, "Bilateral Control of Master-Slave Manipulators for Ideal Kinesthetic Coupling - Formulation and Experiment," *IEEE Trans. on Robotics and Automation,* Vol. 10, No. 5, pp. 605-620 (1994).

A Proof of Theorem 1

Lemma 1 *Let the auxiliary functions $L_1(t), L_2(t) \in \mathbb{R}$ be defined as follows*

$$L_1 \triangleq r^T \left(N_d - \beta_1 sgn(e_2)\right) \tag{60}$$
$$L_2 \triangleq -\beta_2 \dot{e}_2^T sgn(e_2)$$

where β_1 and β_2 were introduced in (29). Provided β_1 is selected according to the following sufficient condition

$$\beta_1 > \varsigma_1 + \frac{1}{\alpha_1} \varsigma_2 \tag{61}$$

where ς_1 and ς_2 are given in (32), and α_1 is introduced in (16), then

$$\int_{t_0}^t L_1(\tau) d\tau \leq \xi_{b1} \qquad \int_{t_0}^t L_2(\tau) d\tau \leq \xi_{b2} \tag{62}$$

where the positive constants $\xi_{b1}, \xi_{b2} \in \mathbb{R}$ are defined as

$$\xi_{b1} \triangleq \beta_1 \sum_{i=1}^{2n} |e_{2i}(t_0)| - e_2^T(t_0) N_d(t_0) \tag{63}$$

$$\xi_{b2} \triangleq \beta_2 \sum_{i=1}^{2n} |e_{2i}(t_0)|. \tag{}$$

Proof. After substituting (16) into (60) and then integrating, the following expression can be obtained

$$\int_{t_0}^t L_1(\tau) d\tau = \alpha_1 \int_{t_0}^t e_2^T(\tau) \left[N_d(\tau) - \beta_1 sgn(e_2(\tau))\right] d\tau \tag{64}$$
$$+ \int_{t_0}^t \frac{de_2^T(\tau)}{d\tau} N_d(\tau) d\tau - \beta_1 \int_{t_0}^t \frac{de_2^T(\tau)}{d\tau} sgn(e_2(\tau)) d\tau.$$

After evaluating the second integral on the right side of (64) by parts and evaluating the third integral, the following expression is obtained

$$\int_{t_0}^t L_1 d\tau = \alpha_1 \int_{t_0}^t e_2^T \left(N_d - \frac{1}{\alpha_1} \frac{dN_d}{d\tau} - \beta_1 sgn(e_2)\right) d\tau$$
$$+ e_2^T(t) N_d(t) - \beta_1 \sum_{i=1}^{2n} |e_{2i}(t)| + \xi_{b1}. \tag{65}$$

The expression in (65) can be upper bounded as follows

$$\int_{t_0}^t L_1 d\tau \leqslant \alpha_1 \int_{t_0}^t \sum_{i=1}^{2n} |e_{2i}(\tau)| \left(|N_{d_i}(\tau)| + \frac{1}{\alpha_1} \left|\frac{dN_{d_i}(\tau)}{d\tau}\right| - \beta_1\right) d\tau \tag{66}$$
$$+ \sum_{i=1}^{2n} |e_{2i}(t)| \left(|N_{d_i}(t)| - \beta_1\right) + \xi_{b1}.$$

20

If β_1 is chosen according to (34), then the first inequality in (62) can be proven from (66). The second inequality in (62) can be obtained by integrating the expression for $L_2(t)$ introduced in (60) as follows

$$
\begin{aligned}
\int_{t_0}^t L_2(\tau)d\sigma &= -\beta_2 \int_{t_0}^t \dot{e}_2^T(\tau)sgn(e_2(\tau))d\tau \\
&= \xi_{b2} - \beta_2 \sum_{i=1}^{2n} |e_{2i}(t)| \leq \xi_{b2}. \quad \blacksquare
\end{aligned}
\tag{67}
$$

The following is the proof of Theorem 1.

Proof. Let the auxiliary functions $P_1(t)$, $P_2(t) \in \mathbb{R}$ be defined as follows

$$
P_1(t) \triangleq \xi_{b1} - \int_{t_0}^t L_1(\tau)d\tau \geq 0
\tag{68}
$$

$$
P_2(t) \triangleq \xi_{b2} - \int_{t_0}^t L_2(\tau)d\tau \geq 0
\tag{69}
$$

where $\xi_{b1}, L_1(t), \xi_{b2}$, and $L_2(t)$ were defined in (60) and (63). The results from Lemma 1 can be used to show that $P_1(t)$ and $P_2(t)$ are non-negative. Let $V(y,t) \in \mathbb{R}$ denote the following nonnegative function

$$
V \triangleq \frac{1}{2}e_1^T e_1 + \frac{1}{2}e_2^T e_2 + \frac{1}{2}r^T \bar{M}r + P_1 + P_2
\tag{70}
$$

where $y(t) \in \mathbb{R}^{6n+2}$

$$
y(t) \triangleq \begin{bmatrix} z^T & \sqrt{P_1} & \sqrt{P_2} \end{bmatrix}^T
\tag{71}
$$

where the composite vector $z(\cdot) \in \mathbb{R}^{6n}$ is defined as follows

$$
z \triangleq \begin{bmatrix} e_1^T & e_2^T & r^T \end{bmatrix}^T.
\tag{72}
$$

Note that (70) is bounded by

$$
W_1(y) \leq V(y,t) \leq W_2(y)
\tag{73}
$$

where

$$
W_1(y) = \lambda_1 \|y(t)\|^2 \quad W_2(y) = \lambda_2 \|y(t)\|^2
\tag{74}
$$

where $\lambda_1 \triangleq \frac{1}{2}\min\{1, \bar{m}_1\}$ and $\lambda_2 \triangleq \max\{1, \frac{1}{2}\bar{m}_2\}$ where $\bar{m}_1$ and $\bar{m}_2$ were introduced in (15).

After taking the time derivative of (70) the following expression can be obtained

$$
\begin{aligned}
\dot{V} &= -\alpha_2 e_1^T e_1 - \alpha_1 e_2^T e_2 - r^T(k_s + 1)r \\
&\quad + e_1^T e_2 + r^T \tilde{N} - r^T \beta_2 sgn(e_2) + \beta_2 \dot{e}_2^T sgn(e_2)
\end{aligned}
\tag{75}
$$

where (16), (17), (31), (68), and (69) were utilized. To facilitate the subsequent analysis, the following inequality can be developed from (26) - (28) (see Appendix F for further details)

$$
\tilde{N} \leq \rho(\|z\|)\|z\|
\tag{76}
$$

21

where $\rho(\cdot)$ is a positive, non-decreasing function. By utilizing (16), (76), and the triangle inequality, $\dot{V}(t)$ can be upper bounded as follows

$$
\begin{aligned}
\dot{V} \leq &\ -\alpha_2 e_1^T e_1 - \alpha_1 e_2^T e_2 - r^T (k_s + 1) r \\
&\ + e_1^T e_1 + e_2^T e_2 + \rho(\|z\|) \|r\| \|z\| - \alpha_1 e_2^T \beta_2 sgn(e_2).
\end{aligned}
\tag{77}
$$

By utilizing (72), $\dot{V}(t)$ of (77) can be upper bounded as follows

$$
\dot{V} \leq -\lambda_3 \|z\|^2 - k_s \|r\|^2 + \rho(\|z\|) \|r\| \|z\| - \alpha_1 \beta_2 \sum_{i=1}^{2n} |e_{2i}|
\tag{78}
$$

where $\lambda_3 \triangleq \min \{\alpha_1 - 1, \alpha_2 - 1, 1\}$. After completing the squares for the second and third term on the right side of (78), the following expression can be obtained

$$
\dot{V} \leq - \left(\lambda_3 - \frac{\rho^2(\|z\|)}{4k_s} \right) \|z\|^2 - \alpha_1 \beta_2 \sum_{i=1}^{2n} |e_{2i}|.
\tag{79}
$$

Provided α_1 and α_2 are selected to be greater than 2 and k_s is selected according to the following sufficient condition

$$
k_s \geq \frac{\rho^2(\|z\|)}{4\lambda_3} \quad \text{or} \quad \|z\| \leq \rho^{-1} \left(2\sqrt{k_s \lambda_3} \right)
\tag{80}
$$

then the following inequality can be developed

$$
\dot{V} \leq W(y) - \alpha_1 \beta_2 \sum_{i=1}^{2n} |e_{2i}|
\tag{81}
$$

where $W(y) \in \mathbb{R}$ denotes the following nonpositive function

$$
W(y) \triangleq -\beta_0 \|z\|^2
\tag{82}
$$

where $\beta_0 \in \mathbb{R}$ denotes a positive constant. From (70)-(74) and (79)-(82) the regions D and S can be defined as follows

$$
\mathcal{D} \triangleq \left\{ y \in \mathbb{R}^{6n+2} \mid \|y\| < \rho^{-1} \left(2\sqrt{k_s \lambda_3} \right) \right\}
\tag{83}
$$

$$
\mathcal{S} \triangleq \left\{ y \in \mathcal{D} \mid W_2(y) < \lambda_1 \left(\rho^{-1} \left(2\sqrt{k_s \lambda_3} \right) \right)^2 \right\}.
\tag{84}
$$

The region of attraction in (84) can be made arbitrarily large to include any initial conditions by increasing the control gain k_s (i.e. a semi-global stability result). Specifically, (74) and the region defined in (84) can be used to calculate the region of attraction as follows

$$
\begin{aligned}
W_2(y(t_0)) \ &< \ \lambda_1 \left(\rho^{-1} \left(2\sqrt{k_s \lambda_3} \right) \right)^2 \\
&\implies \ \|y(t_0)\| < \sqrt{\frac{\lambda_1}{\lambda_2}} \rho^{-1} \left(2\sqrt{k_s \lambda_3} \right),
\end{aligned}
\tag{85}
$$

22

which can be rearranged as

$$k_s \geq \frac{1}{4\lambda_3} \rho^2 \left(\sqrt{\frac{\lambda_2}{\lambda_1}} \|y(t_0)\| \right). \tag{86}$$

By using (72), (63), and (71) an explicit expression for $\|y(t_0)\|$ can be written as

$$\begin{aligned} \|y(t_0)\|^2 &= \|e_1(t_0)\|^2 + \|e_2(t_0)\|^2 \\ &\quad + \|r(t_0)\|^2 + \xi_{b1} + \xi_{b2}. \end{aligned} \tag{87}$$

From (70), (81), and (84)-(86), it is clear that $V(y,t) \in \mathcal{L}_\infty \; \forall y(t_0) \in \mathcal{S}$; hence $e_1(t)$, $e_2(t)$, $r(t)$, $z(t)$, $y(t) \in \mathcal{L}_\infty \; \forall y(t_0) \in \mathcal{S}$. From (81) it is easy to show that $e_2(t) \in \mathcal{L}_1 \; \forall y(t_0) \in \mathcal{S}$. The fact that $e_2(t) \in \mathcal{L}_1 \; \forall y(t_0) \in \mathcal{S}$ can be used along with (17) to determine that $e_1(t), \dot{e}_1(t) \in \mathcal{L}_1 \; \forall y(t_0) \in \mathcal{S}$. From (7), (18) and the assumption that $q_d(t) \in \mathcal{L}_\infty$, it is clear that $x(t)$, $q(t) \in \mathcal{L}_\infty \; \forall y(t_0) \in \mathcal{S}$. From (16) and (17) it is also clear that $\dot{e}_2(t)$, $\dot{e}_1(t) \in \mathcal{L}_\infty \; \forall y(t_0) \in \mathcal{S}$. Using these boundedness statements, it is clear that both $\dot{\bar{u}}(t) \in \mathcal{L}_\infty \; \forall y(t_0) \in \mathcal{S}$. From the time derivative of (17), and using the assumption that $\ddot{q}_d(t) \in \mathcal{L}_\infty$ along with (23), it is clear that $\bar{u}(t) \in \mathcal{L}_\infty \; \forall y(t_0) \in \mathcal{S}$. The previous boundedness statements can be used along with (31), (76), and Remark 2 to prove that $\dot{r}(t) \in \mathcal{L}_\infty$ $\forall y(t_0) \in \mathcal{S}$. These bounding statements can be used along with the time derivative of (82) to prove that $\dot{W}(y(t)) \in \mathcal{L}_\infty \; \forall y(t_0) \in S$; hence, $W(y(t))$ is uniformly continuous. Standard signal chasing arguments can be used to prove all remaining signals are bounded. A direct application of Theorem 8.4 in [10] can now be used to prove that $\|z(t)\| \to 0$ as $t \to \infty \; \forall y(t_0) \in \mathcal{S}$. From (72), it is also clear that $\|r(t)\| \to 0$ as $t \to \infty \; \forall y(t_0) \in \mathcal{S}$. Based on the definitions give in (16) - (18), standard linear analysis tools can be used to prove that if $\|r(t)\| \to 0$ then $\|\dot{e}_2(t)\|$, $\|e_2(t)\|$, $\|\dot{e}_1(t)\|$, $\|e_1(t)\| \to 0$ as $t \to \infty \; \forall y(t_0) \in \mathcal{S}$. Based on the definition of $x(t)$ in (7) and $e_1(t)$ in (18), it is clear that if $\|e_1(t)\| \to 0$ then $\|q_1(t) - q_2(t)\| \to 0$ and $q_1(t) + q_2(t) \to q_d(t)$. ∎

B Proof of Theorem 2

Proof. Let $V_p(t) \in \mathbb{R}$ denote the following nonnegative, bounded function

$$V_p \triangleq \frac{1}{2} \dot{q}_d^T M_T \dot{q}_d + \frac{1}{2} q_d^T K_T q_d. \tag{88}$$

After taking the time derivative of (88), the following simplified expression can be obtained

$$\dot{V}_p = \dot{q}_d^T \bar{F}_2 - \dot{q}_d^T B_T \dot{q}_d \tag{89}$$

where (20) was utilized. Based on the fact that B_T is a constant positive definite, diagonal matrix, the following inequality can be developed

$$\dot{V}_p \leq \dot{q}_d^T \bar{F}_2. \tag{90}$$

After integrating of both sides of (90), the following inequality can be developed

$$-c_2 \leq V_p(t) - V_p(t_0) \leq \int_{t_0}^{t} \dot{q}_d^T(\sigma) \bar{F}_2(\sigma) d\sigma \tag{91}$$

where $c_2 \in \mathbb{R}$ is a positive constant (since $V_p(t)$ is bounded from the trajectory generation system in (20)).

By using the transformation in (7), the left side of (5) can be expressed as

$$\int_{t_0}^{t} \dot{q}^T(\tau) \begin{bmatrix} \gamma F_1(\tau) \\ F_2(\tau) \end{bmatrix} d\tau = \int_{t_0}^{t} \dot{x}^T \bar{F} d\tau. \tag{92}$$

By substituting the time derivative of (18) into (92), the following expression can be obtained

$$\int_{t_0}^{t} \dot{x}^T(\tau) \bar{F}(\tau) d\tau = \int_{t_0}^{t} \dot{q}_d^T(\tau) \bar{F}_2(\tau) d\tau - \int_{t_0}^{t} \dot{e}_1^T(\tau) \bar{F}(\tau) d\tau \tag{93}$$

where (19) was utilized. Based on (91), it is clear that $\int_{t_0}^{t} \dot{q}_d^T(\tau) \bar{F}_2(\tau) d\tau$ is lower bounded by $-c_2$, where c_2 was defined as a positive constant. The fact that $\dot{e}_1(t) \in \mathcal{L}_1$ from the proof for Theorem 1 and the assumption that $\bar{F}(t) \in \mathcal{L}_\infty$ can be used to show that the second integral of (93) is bounded. Hence, these facts can be applied to (92) and (93) to prove that

$$\int_{t_0}^{t} \dot{q}^T(\tau) \begin{bmatrix} \gamma F_1(\tau) \\ F_2(\tau) \end{bmatrix} d\tau \geq -c_3^2 \tag{94}$$

where $c_3 \in \mathbb{R}$ is a positive constant. ∎

C   UMIF Desired Trajectory Stability Analysis

Proof. Let $V_1(t) \in \mathbb{R}$ denote the following nonnegative function

$$V_1 \triangleq \frac{1}{2} e_2^T e_2 + \frac{1}{2} r^T r + P_1 + P_2. \tag{95}$$

Based on (95) and the closed loop error systems in (56), the proof of Theorem 3 can be followed directly to prove that $e_1(t), e_2(t), r(t), \hat{F}(t), \dot{\hat{F}}(t) \in \mathcal{L}_\infty$ as well as that $e_1(t), e_2(t)$, and $r(t) \to 0$ as $t \to \infty$ regardless of whether or not $x_d(t), \dot{x}_d(t), \ddot{x}_d(t) \in \mathcal{L}_\infty$. Therefore the fact that $\hat{F}(t) \in \mathcal{L}_\infty$ can be used in the subsequent analysis. As a means to prove that $x_d(t), \dot{x}_d(t), \ddot{x}_d(t) \in \mathcal{L}_\infty$, let $V_2(t) \in \mathbb{R}$ denote the following nonnegative function

$$V_2 \triangleq V_3 + L \tag{96}$$

where $V_3(t) \in \mathbb{R}$ denotes the following nonnegative function

$$V_3 \triangleq \frac{1}{2} \dot{x}_d^T \bar{M} \dot{x}_d + \frac{1}{2} x_d^T K_T x_d \tag{97}$$

where $x_d(t), \dot{x}_d(t)$ were defined in (40), where K_T was defined in (39), and $\bar{M}(x)$ was defined in (10). The expression given in (97) can be lower bounded by the auxiliary function, $L(\bar{x}) \in \mathbb{R}$, defined as follows

$$L \triangleq \frac{2\varepsilon \dot{x}_d^T \bar{M} x_d}{1 + 2 x_d^T x_d} \leq V_3(t) \tag{98}$$

where $\varepsilon \in \mathbb{R}$ is a positive bounding constant selected according to the following inequality

$$0 < \varepsilon < \frac{\min\{\bar{m}_1, \lambda_{\min}\{K_T\}\}}{2m_{L\infty}} \tag{99}$$

where $\lambda_{\min}\{K_T\} \in \mathbb{R}$ denotes the minimum eigenvalue of K_T, $\bar{m}_1$ was defined in (15) and $m_{L\infty} \in \mathbb{R}$ denotes the induced infinity norm of the bounded matrix $\bar{M}(x)$. From (98) it is clear that $V_2(t)$ is a non-negative function. Also, $\bar{x}(t) \in \mathbb{R}^{4n}$ is defined as

$$\bar{x} \triangleq [\ x_d^T \quad \dot{x}_d^T\ ]^T. \tag{100}$$

The expression in (96) satisfies the following inequalities

$$\bar{\lambda}_1 \|\bar{x}\|^2 \le V_2(\bar{x}) \le \bar{\lambda}_2 \|\bar{x}\|^2 \tag{101}$$

where $\bar{\lambda}_1, \bar{\lambda}_2 \in \mathbb{R}$ are positive constants defined as follows, provided ε is selected sufficiently small

$$\bar{\lambda}_1 \triangleq \frac{1}{2}\min\{\bar{m}_1, \lambda_{\min}\{K_T\}\} - \varepsilon\xi_c \tag{102}$$

$$\bar{\lambda}_2 \triangleq \frac{1}{2}\max\{\bar{m}_2, \lambda_{\max}\{K_T\}\} + \varepsilon\xi_c$$

where $\bar{m}_1$ and $\bar{m}_2$ were introduced in (15), and $\lambda_{\max}\{K_T\} \in \mathbb{R}$ denotes the maximum eigenvalue of K_T. In (102), $\xi_c \in \mathbb{R}$ is a positive constant defined as follows

$$\xi_c = \max\left\{\frac{2m_{L\infty}}{\delta_a}, 2m_{L\infty}\delta_a\right\} \tag{103}$$

where $\delta_a \in \mathbb{R}$ is some positive constant, and $m_{L\infty}$ was introduced in (99).

To facilitate the subsequent analysis, the time derivative of (98) can be determined as follows

$$\dot{L} = \frac{2\varepsilon\ddot{x}_d^T\bar{M}x_d + 2\varepsilon\dot{x}_d^T\dot{\bar{M}}x_d + 2\varepsilon\dot{x}_d^T\bar{M}\dot{x}_d}{1 + 2x_d^Tx_d}$$
$$-\frac{2\varepsilon\left(\dot{x}_d^T\bar{M}x_d\right)4x_d^T\dot{x}_d}{(1 + 2x_d^Tx_d)^2}. \tag{104}$$

After utilizing (39), the expression in (104) can be written as

$$\dot{L} = -\frac{2\varepsilon x_d^T K_T x_d}{1 + 2x_d^T x_d} - \frac{2\varepsilon x_d^T B_T \dot{x}_d}{1 + 2x_d^T x_d} + \frac{2\varepsilon x_d^T \hat{F}}{1 + 2x_d^T x_d}$$
$$+\frac{\varepsilon x_d^T \dot{\bar{M}} \dot{x}_d}{1 + 2x_d^T x_d} + \frac{2\varepsilon\dot{x}_d^T\bar{M}\dot{x}_d}{1 + 2x_d^T x_d} - \frac{2\varepsilon\left(\dot{x}_d^T\bar{M}x_d\right)4x_d^T\dot{x}_d}{(1 + 2x_d^T x_d)^2}. \tag{105}$$

The signal in (105) can be upper bounded as follows

$$\dot{L} \le -\frac{2\varepsilon\lambda_{\min}\{K_T\}}{1 + 2x_d^T x_d}\|x_d\|^2 + \frac{2\varepsilon\lambda_{\max}\{B_T\}}{1 + 2x_d^T x_d}\left[\|x_d\|^2 + \|\dot{x}_d\|^2\right]$$
$$+\frac{2\varepsilon}{1 + 2x_d^T x_d}\left[\delta_2\|x_d\|^2 + \frac{1}{\delta_2}\|\hat{F}\|^2\right] + \varepsilon\xi_3\xi_{\bar{m}}\|\dot{x}_d\|^2 + \varepsilon\xi_{\bar{m}}\xi_{\dot{e}} \tag{106}$$
$$+\frac{\varepsilon\xi_{\bar{m}}\xi_{\dot{e}}}{1 + 2x_d^T x_d}\|\dot{x}_d\|^2 + \frac{2\varepsilon\bar{m}_2}{1 + 2x_d^T x_d}\|\dot{x}_d\|^2 + 8\varepsilon\bar{m}_2\|\dot{x}_d\|^2$$

25

where the following properties were utilized

$$-\frac{2\varepsilon x_d^T K_T x_d}{1 + 2x_d^T x_d} \leq -\frac{2\varepsilon \lambda_{\min}\{K_T\}}{1 + 2x_d^T x_d} \|x_d\|^2 \tag{107}$$

$$-\frac{2\varepsilon x_d^T B_T \dot{x}_d}{1 + 2x_d^T x_d} \leq \frac{2\varepsilon \lambda_{\max}\{B_T\}}{1 + 2x_d^T x_d} \left[\|x_d\|^2 + \|\dot{x}_d\|^2\right] \tag{108}$$

$$\frac{2\varepsilon x_d^T \hat{F}}{1 + 2x_d^T x_d} \leq \frac{2\varepsilon}{1 + 2x_d^T x_d} \left[\delta_2 \|x_d\|^2 + \frac{1}{\delta_2} \left\|\hat{F}\right\|^2\right] \tag{109}$$

$$\frac{\varepsilon x_d^T \dot{\bar{M}} \dot{x}_d}{1 + 2x_d^T x_d} \leq \varepsilon \xi_3 \xi_{\bar{m}} \|\dot{x}_d\|^2 + \varepsilon \xi_{\bar{m}} \xi_{\dot{e}} + \frac{\varepsilon \xi_{\bar{m}} \xi_{\dot{e}}}{1 + 2x_d^T x_d} \|\dot{x}_d\|^2 \tag{110}$$

$$\frac{2\varepsilon \dot{x}_d^T \bar{M} \dot{x}_d}{1 + 2x_d^T x_d} \leq \frac{2\varepsilon \bar{m}_2}{1 + 2x_d^T x_d} \|\dot{x}_d\|^2 \tag{111}$$

$$-\frac{2\varepsilon \left(\dot{x}_d^T \bar{M} x_d\right) 4x_d^T \dot{x}_d}{\left(1 + 2x_d^T x_d\right)^2} \leq 8\varepsilon \bar{m}_2 \|\dot{x}_d\|^2 \tag{112}$$

$$\frac{\|x_d\|^2}{1 + 2x_d^T x_d} \leq 1 \tag{113}$$

$$\frac{\|x_d\|^2}{\left(1 + 2x_d^T x_d\right)^2} \leq 1. \tag{114}$$

In (109), $\delta_2 \in \mathbb{R}$ denotes a positive bounding constant. In (110), $\xi_3 \in \mathbb{R}$ denotes a positive bounding constant defined as

$$\frac{\|x_d\|}{1 + 2x_d^T x_d} \leq \xi_3 \tag{115}$$

and $\xi_{\bar{m}}$, $\xi_{\dot{e}} \in \mathbb{R}$ denote positive bounding constants defined as

$$\left\|\dot{\bar{M}}\right\| \leq \xi_{\bar{m}} \left(\|\dot{x}_d\| + \xi_{\dot{e}}\right). \tag{116}$$

The inequality in (116) is obtained by using the facts that the inertia matrix is second order differentiable and that $e_1(t) \in \mathcal{L}_\infty$, (see proof of Theorem 3). In (111) and (112), $\bar{m}_2 \in \mathbb{R}$ is a positive constant defined in (15).

Based on the development in (104)-(114), the time derivative of (96) can be upper bounded as follows

$$\begin{aligned}
\dot{V}_2 \leq \; & -\lambda_{\min}\{B_T\} \|\dot{x}_d\|^2 - \frac{2\varepsilon \lambda_{\min}\{K_T\}}{1 + 2x_d^T x_d} \|x_d\|^2 \\
& + \frac{2\varepsilon \lambda_{\max}\{B_T\}}{1 + 2x_d^T x_d} \left[\|x_d\|^2 + \|\dot{x}_d\|^2\right] \\
& + \delta_1 \|\dot{x}_d\|^2 + \frac{1}{\delta_1} \left\|\hat{F}\right\|^2 + \frac{2\varepsilon}{1 + 2x_d^T x_d} \left[\delta_2 \|x_d\|^2 + \frac{1}{\delta_2} \left\|\hat{F}\right\|^2\right] \\
& + \varepsilon \xi_3 \xi_{\bar{m}} \|\dot{x}_d\|^2 + \varepsilon \xi_{\bar{m}} \xi_{\dot{e}} + \frac{\varepsilon \xi_{\bar{m}} \xi_{\dot{e}}}{1 + 2x_d^T x_d} \|\dot{x}_d\|^2 \\
& + \frac{2\varepsilon \bar{m}_2}{1 + 2x_d^T x_d} \|\dot{x}_d\|^2 + 8\varepsilon \bar{m}_2 \|\dot{x}_d\|^2
\end{aligned} \tag{117}$$

where (39), (106), and the following inequalities were utilized

$$-\dot{x}_d^T B_T \dot{x}_d \leq -\lambda_{\min}\{B_T\} \|\dot{x}_d\|^2$$
$$\dot{x}_d^T \hat{F} \leq \delta_1 \|\dot{x}_d\|^2 + \frac{1}{\delta_1} \left\|\hat{F}\right\|^2$$

where $\delta_1 \in \mathbb{R}$ denotes a positive bounding constant. The expression in (117) can be simplified as follows

$$
\begin{aligned}
\dot{V}_2 \leq &- \|\dot{x}_d\|^2 \left[\lambda_{\min}\{B_T\} - \delta_1 - \frac{2\varepsilon\lambda_{\max}\{B_T\}}{1 + 2x_d^T x_d} - \varepsilon\xi_3\xi_{\bar{m}} - \frac{\varepsilon\xi_{\bar{m}}\xi_{\dot{e}}}{1 + 2x_d^T x_d} - \frac{2\varepsilon\bar{m}_2}{1 + 2x_d^T x_d} - 8\varepsilon\bar{m}_2\right] \\
&- \|x_d\|^2 \left[\frac{2\varepsilon\lambda_{\min}\{K_T\}}{1 + 2x_d^T x_d} - \frac{2\varepsilon\lambda_{\max}\{B_T\}}{1 + 2x_d^T x_d} - \frac{2\varepsilon\delta_2}{1 + 2x_d^T x_d}\right] \\
&+ \left[\frac{1}{\delta_1} \left\|\hat{F}\right\|^2\right] + \left[\frac{2\varepsilon}{1 + 2x_d^T x_d}\right] \left[\frac{1}{\delta_2} \left\|\hat{F}\right\|^2\right] + \varepsilon\xi_{\bar{m}}\xi_{\dot{e}}\right].
\end{aligned}
\tag{118}
$$

Provided B_T, δ_1, δ_2, ε, and K_T are selected to satisfy the following sufficient conditions

$$\lambda_{\min}\{B_T\} > \delta_1 + \varepsilon\left(2\lambda_{\max}\{B_T\} + \xi_3\xi_{\bar{m}} + \xi_{\bar{m}}\xi_{\dot{e}} + 10\bar{m}_2\right)$$
$$\lambda_{\min}\{K_T\} > \lambda_{\max}\{B_T\} + \delta_2$$

the expression in (118) can be upper bounded as follows

$$\dot{V}_2 \leq -\frac{\min\{\gamma_a, \gamma_b\}}{\bar{\lambda}_2} V_3 + \epsilon_2 \tag{119}$$

where (100) was utilized, and γ_a, γ_b, $\epsilon_2 \in \mathbb{R}$ denote positive bounding constants.

From (96) - (98), and (101), and that $\hat{F}(t) \in \mathcal{L}_\infty$, the expression in (119) can be used with the result from [5] to prove that $\bar{x}(t), x_d(t)$, $\dot{x}_d(t) \in \mathcal{L}_\infty$. Based on (39), and the fact that $\bar{M}(x)$, $\dot{\bar{M}}(x, \dot{x})$, and $\hat{F}(t) \in \mathcal{L}_\infty$ then $\ddot{x}_d(t) \in \mathcal{L}_\infty$. ∎

D   Proof of Theorem 3

Lemma 2 *Let the auxiliary functions $L_1(t), L_2(t) \in \mathbb{R}$ be defined as follows*

$$L_1 \triangleq -r^T\left(\dot{\bar{F}} + \beta_1 sgn(e_2)\right) \tag{120}$$
$$L_2 \triangleq -\beta_2\dot{e}_2^T sgn(e_2)$$

where β_1 and β_2 are defined in (54). Provided β_1 is selected according to the following sufficient condition

$$\beta_1 > \varsigma_3 + \varsigma_4, \tag{121}$$

where ς_3 and ς_4 were introduced in (57), then

$$\int_{t_0}^t L_1(\tau)d\tau \leq \xi_{b1} \qquad \int_{t_0}^t L_2(\tau)d\tau \leq \xi_{b2} \tag{122}$$

where the positive constants $\xi_{b1}, \xi_{b2} \in \mathbb{R}$ are defined as

$$\xi_{b1} \triangleq \beta_1 \sum_{i=1}^{2n} |e_{2i}(t_0)| - e_2^T(t_0)\left(-\dot{\bar{F}}(t_0)\right) \qquad \xi_{b2} \triangleq \beta_2 \sum_{i=1}^{2n} |e_{2i}(t_0)|. \tag{123}$$

27

Proof. After substituting (44) into (120) and then integrating, the following expression can be obtained

$$\int_{t_0}^{t} L_1(\tau)d\tau \;=\; \int_{t_0}^{t} e_2^T(\tau)\left[-\dot{\bar{F}}(\tau) - \beta_1 sgn(e_2(\tau))\right]d\tau \tag{124}$$

$$+\int_{t_0}^{t} \frac{de_2^T(\tau)}{d\tau}\left(-\dot{\bar{F}}(\tau)\right)d\tau - \beta_1\int_{t_0}^{t}\frac{de_2^T(\tau)}{d\tau}sgn(e_2(\tau))d\tau.$$

After evaluating the second integral on the right side of (124) by parts and evaluating the third integral, the following expression is obtained

$$\int_{t_0}^{t} L_1 d\tau \;=\; \int_{t_0}^{t} e_2^T(\tau)\left(-\dot{\bar{F}}(\tau) + \ddot{\bar{F}}(\tau) - \beta_1 sgn(e_2(\tau))\right)d\tau$$

$$-e_2^T(t)\,\dot{\bar{F}}(t) - \beta_1\sum_{i=1}^{2n}|e_{2i}(t)| + \xi_{b1}. \tag{125}$$

The expression in (125) can be upper bounded as follows

$$\int_{t_0}^{t} L_1 d\tau \;\leqslant\; \int_{t_0}^{t}\sum_{i=1}^{2n}|e_{2i}(\tau)|\left(\left|\dot{\bar{F}}_i(\tau)\right| + \left|\ddot{\bar{F}}_i(\tau)\right| - \beta_1\right)d\tau \tag{126}$$

$$+\sum_{i=1}^{2n}|e_{2i}(t)|\left(\left|\dot{\bar{F}}_i(t)\right| - \beta_1\right) + \xi_{b1}.$$

If β_1 is chosen according to (121), then the first inequality in (122) can be proven from (126). The second inequality in (122) can be obtained by integrating the expression for $L_2(t)$ introduced in (120) as follows

$$\int_{t_0}^{t} L_2(\tau)d\sigma \;=\; -\beta_2\int_{t_0}^{t}\dot{e}_2^T(\tau)sgn(e_2(\tau))d\tau \tag{127}$$

$$=\; \xi_{b2} - \beta_2\sum_{i=1}^{2n}|e_{2i}(t)| \leq \xi_{b2}. \;\blacksquare$$

The following is the proof of Theorem 3.

Proof. Let the auxiliary functions $P_1(t)$, $P_2(t) \in \mathbb{R}$ be defined as follows

$$P_1(t) \triangleq \xi_{b1} - \int_{t_0}^{t} L_1(\tau)d\tau \geq 0 \tag{128}$$

$$P_2(t) \triangleq \xi_{b2} - \int_{t_0}^{t} L_2(\tau)d\tau \geq 0 \tag{129}$$

where $\xi_{b1}, L_1(t), \xi_{b2}$, and $L_2(t)$ were defined in (120) and (123). The results from Lemma 2 can be used to show that $P_1(t)$ and $P_2(t)$ are non-negative. Let $V_1(y,t) \in \mathbb{R}$ denote the following nonnegative function

$$V_1 \triangleq \frac{1}{2}e_2^T e_2 + \frac{1}{2}r^T r + P_1 + P_2 \tag{130}$$

28

where $y(t) \in \mathbb{R}^{4n+2}$ is defined as

$$y(t) \triangleq \begin{bmatrix} e_2^T & r^T & \sqrt{P_1} & \sqrt{P_2} \end{bmatrix}^T. \tag{131}$$

Note that (130) is bounded according to the following inequalities

$$W_3(y) \leq V_1(y, t) \leq W_4(y) \tag{132}$$

where

$$W_3(y) = \lambda_4 \|y(t)\|^2 \qquad W_4(y) = \lambda_5 \|y(t)\|^2 \tag{133}$$

where λ_4, $\lambda_5 \in \mathbb{R}$ are positive bounding constants.

After taking the time derivative of (130), the following expression can be obtained

$$\dot{V}_1 = -e_2^T e_2 - k_s r^T r - \beta_2 e_2^T sgn(e_2) \tag{134}$$

where (44), (56), (128), and (129) were utilized. The expression in (134) can be rewritten as

$$\dot{V}_1 = -\|e_2\|^2 - k_s \|r\|^2 - \beta_2 \sum_{i=1}^{2n} |e_{2i}|. \tag{135}$$

From (130) and (135), it is clear that $V_1(y, t) \in \mathcal{L}_\infty$; hence, $e_2(t) \in \mathcal{L}_\infty \cap \mathcal{L}_2 \cap \mathcal{L}_1$, $r(t) \in \mathcal{L}_\infty \cap \mathcal{L}_2$, and $y(t) \in \mathcal{L}_\infty$. Since $e_2(t)$, $r(t) \in \mathcal{L}_\infty$, (44) and (55) can be used to prove that $\dot{e}_2(t), \hat{\dot{F}}(t) \in \mathcal{L}_\infty$. Given that $e_2(t)$, $r(t)$, $\hat{\dot{F}}(t) \in \mathcal{L}_\infty$ and the assumption that $\bar{F} \in \mathcal{L}_\infty$, (53) can be used to prove that $\dot{r}(t) \in \mathcal{L}_\infty$. Barbalat's Lemma can be utilized to prove

$$\|e_2(t)\|, \|r(t)\| \to 0 \quad as \quad t \to \infty. \tag{136}$$

From (44), (45), (136) and the fact that $\bar{M}(x) \in \mathcal{L}_\infty$, standard linear analysis arguments can be used to prove that $e_1(t)$, $\dot{e}_1(t)$, and $\dot{e}_2(t) \in \mathcal{L}_\infty$, likewise that $e_1(t)$, $\dot{e}_1(t) \in \mathcal{L}_1$, and that

$$\|e_1(t)\|, \|\dot{e}_1(t)\|, \|\dot{e}_2(t)\| \to 0 \quad as \quad t \to \infty. \tag{137}$$

From the fact that $\dot{e}_2(t) \in \mathcal{L}_\infty$ and the assumption that $\bar{F} \in \mathcal{L}_\infty$ it is clear from (51) that $\hat{F}(t) \in \mathcal{L}_\infty$. Since $\hat{F}(t) \in \mathcal{L}_\infty$, (39) and the proof in Appendix C can be used to show that $x_d(t)$, $\dot{x}_d(t)$, $\ddot{x}_d(t) \in \mathcal{L}_\infty$. Using these facts along with (18) and its first time derivative, it is clear that $x(t)$ and $\dot{x}(t) \in \mathcal{L}_\infty$. Since $e_1(t)$, $\dot{e}_1(t)$, $\bar{M}(x)$, $\dot{\bar{M}}(x) \in \mathcal{L}_\infty$, it is clear from (50) that $\bar{T}_1(t) \in \mathcal{L}_\infty$, and using previously stated bounding properties, $\bar{T}(t) \in \mathcal{L}_\infty$. It is also possible to state that $\bar{T}_1(t) \in \mathcal{L}_1$, where (50) was utilized. Based on the definition of $x(t)$ in (42) and the previously stated bounding properties, it is clear that $\|q_1(t) - q_2(t)\| \to 0$ and $q_1(t) + q_2(t) \to q_d(t)$. From these bounding statements and standard signal chasing arguments, all signals can be shown to be bounded. ∎

E   Proof of Theorem 4

Proof. Let $V_{p2}(t) \in \mathbb{R}$ denote the following nonnegative, bounded function

$$V_{p2} \triangleq \frac{1}{2} \dot{x}_d^T \bar{M} \dot{x}_d + \frac{1}{2} x_d^T K_T x_d. \tag{138}$$

After taking the time derivative of (138), the following simplified expression can be obtained

$$\dot{V}_{p2} = \dot{x}_d^T \hat{F} - \dot{x}_d^T B_T \dot{x}_d \tag{139}$$

where (39) was utilized. Based on the fact that B_T is a constant positive definite, diagonal matrix, the following inequality can be developed

$$\dot{V}_{p2} \le \dot{x}_d^T \hat{F}. \tag{140}$$

The following inequality can be developed after integrating (140)

$$-c_4 \le V_{p2}(t) - V_{p2}(t_0) \le \int_{t_0}^t \dot{x}_d^T(\sigma) \hat{F}(\sigma) d\sigma \tag{141}$$

where $c_4 \in \mathbb{R}$ is a positive constant (since $V_{p2}(t)$ is bounded from the trajectory generation system in (39)).

To facilitate the subsequent analysis, the following expression can be obtained from integration by parts

$$\int_{t_0}^t \bar{M} \ddot{e}_1(\tau) d\tau = \bar{M} \dot{e}_1(t) - \bar{M} \dot{e}_1(t_0) - \int_{t_0}^t \dot{\bar{M}} \dot{e}_1(\tau) d\tau. \tag{142}$$

Since $\bar{M}(x)$, $\dot{\bar{M}}(x, \dot{x})$, $\dot{e}_1(t) \in \mathcal{L}_\infty$, and $\dot{e}_1(t) \in \mathcal{L}_1$, then $\int_{t_0}^t \bar{M} \ddot{e}_1(\tau) d\tau \in \mathcal{L}_\infty$. After integrating (48) as follows

$$\int_{t_0}^t \tilde{F}(\tau) d\tau = - \int_{t_0}^t \bar{M} \ddot{e}_1(\tau) d\tau - \int_{t_0}^t \bar{T}_1(\tau) d\tau \tag{143}$$

and using the fact that $\bar{T}_1(t) \in \mathcal{L}_1$ (see proof of Theorem 3) and the fact that $\int_{t_0}^t \bar{M} \ddot{e}_1(\tau) d\tau \in \mathcal{L}_\infty$, it is clear that $\tilde{F} \in \mathcal{L}_1$, where $\tilde{F}(t) \triangleq \bar{F}(t) - \hat{F}(t)$.

By using the transformation in (42), the expression in (5) can be rewritten as follows

$$\int_{t_0}^t \dot{q}^T(\tau) \begin{bmatrix} \gamma F_1(\tau) \\ F_2(\tau) \end{bmatrix} d\tau = \int_{t_0}^t \dot{x}^T \bar{F} d\tau - \int_{t_0}^t \begin{bmatrix} \dot{x}_{d1}^T & 0_n^T \end{bmatrix} \bar{F} d\tau. \tag{144}$$

After substituting for the definition of $\tilde{F}(t)$ and the time derivative of (18) into (144) for $\bar{F}(t)$ and $\dot{x}(t)$, respectively, the following expression can be obtained

$$\int_{t_0}^t \dot{x}^T \bar{F} d\tau - \int_{t_0}^t \begin{bmatrix} \dot{x}_{d1}^T & 0_n^T \end{bmatrix} \bar{F} d\tau = \int_{t_0}^t \dot{x}_{d2}^T(\tau) \tilde{F}_2(\tau) d\tau + \int_{t_0}^t \dot{x}_{d2}^T(\tau) \hat{F}_2(\tau) d\tau \\ - \int_{t_0}^t \dot{e}_1^T(\tau) \tilde{F}(\tau) d\tau - \int_{t_0}^t \dot{e}_1^T(\tau) \hat{F}(\tau) d\tau. \tag{145}$$

Since $\dot{x}_d(t) = \begin{bmatrix} \dot{x}_{d_1}^T(t) & \dot{x}_{d_2}^T(t) \end{bmatrix}^T \in \mathcal{L}_\infty$ and $\tilde{F}(t) = \begin{bmatrix} \tilde{F}_1^T(t) & \tilde{F}_2^T(t) \end{bmatrix}^T \in \mathcal{L}_1$, it is clear that the first integral expression in (145) is bounded and from (143) a lower negative bound exists. Based on (141), it is clear that the second integral expression in (145) is bounded and a lower negative bound exists. Since $\dot{e}_1(t) \in \mathcal{L}_\infty$ and $\tilde{F}(t) \in \mathcal{L}_1$, it is possible to show that the third integral in (145) is also bounded and a lower negative bound exists. Finally, because $\dot{e}_1(t) \in \mathcal{L}_1$ and $\hat{F}(t) \in \mathcal{L}_\infty$, it is possible to show that the fourth integral in (145) is also bounded and a lower negative bound exists. Hence, these facts can be applied to (144) and (145) to prove that

$$\int_{t_0}^t \dot{q}^T(\tau) \begin{bmatrix} \gamma F_1(\tau) \\ F_2(\tau) \end{bmatrix} d\tau \ge -c_5^2 \tag{146}$$

where $c_5 \in \mathbb{R}$ is a positive constant. ∎

F   Upper Bound Development for MIF Analysis

To simplify the following derivations, (27) can be rewritten as follows

$$N \triangleq N(x, \dot{x}, \ddot{x}, e_1, e_2, r, \dddot{x}_d) = \bar{M}\dddot{x}_d \tag{147}$$
$$+ \dot{\bar{M}}\ddot{x} + \frac{d}{dt}\left[\bar{C}\dot{x} + \bar{B}\dot{x}\right] + e_2$$
$$+ \bar{M}(\alpha_1 + \alpha_2)r - \bar{M}(\alpha_1^2 + \alpha_1\alpha_2 + \alpha_2^2)e_2$$
$$+ \bar{M}\alpha_2^3 e_1 + \frac{1}{2}\dot{\bar{M}}r$$

where (16) and (17) were utilized. To further facilitate the subsequent analysis, the following terms, $N(x, \dot{x}_d, \ddot{x}_d, 0, 0, 0, \dddot{x}_d)$, $N(x, \dot{x}, \ddot{x}_d, 0, 0, 0, \dddot{x}_d)$, $N(x, \dot{x}, \ddot{x}, 0, 0, 0, \dddot{x}_d)$, $N(x, \dot{x}, \ddot{x}, e_1, 0, 0, \dddot{x}_d)$ and

$N(x, \dot{x}, \ddot{x}, e_1, e_2, 0, \dddot{x}_d)$ are added and subtracted to the right-hand side of (26) as follows

$$\begin{aligned}
\tilde{N} &= [N(x, \dot{x}_d, \ddot{x}_d, 0, 0, 0, \dddot{x}_d) - N_d(x_d, \dot{x}_d, \ddot{x}_d, 0, 0, 0, \dddot{x}_d)] \\
&+ [N(x, \dot{x}, \ddot{x}_d, 0, 0, 0, \dddot{x}_d) - N(x, \dot{x}_d, \ddot{x}_d, 0, 0, 0, \dddot{x}_d)] \\
&+ [N(x, \dot{x}, \ddot{x}, 0, 0, 0, \dddot{x}_d) - N(x, \dot{x}, \ddot{x}_d, 0, 0, 0, \dddot{x}_d)] \\
&+ [N(x, \dot{x}, \ddot{x}, e_1, 0, 0, \dddot{x}_d) - N(x, \dot{x}, \ddot{x}, 0, 0, 0, \dddot{x}_d)] \\
&+ [N(x, \dot{x}, \ddot{x}, e_1, e_2, 0, \dddot{x}_d) - N(x, \dot{x}, \ddot{x}, e_1, 0, 0, \dddot{x}_d)] \\
&+ [N(x, \dot{x}, \ddot{x}, e_1, e_2, r, \dddot{x}_d) - N(x, \dot{x}, \ddot{x}, e_1, e_2, 0, \dddot{x}_d)].
\end{aligned} \tag{148}$$

After applying the Mean Value Theorem to each bracketed term of (148), the following expression can be obtained

$$\begin{aligned}
\tilde{N} &= \left.\frac{\partial N(\sigma_1, \dot{x}_d, \ddot{x}_d, 0, 0, 0, \dddot{x}_d)}{\partial \sigma_1}\right|_{\sigma_1 = v_1} (x - x_d) \\
&+ \left.\frac{\partial N(x, \sigma_2, \ddot{x}_d, 0, 0, 0, \dddot{x}_d)}{\partial \sigma_2}\right|_{\sigma_2 = v_2} (\dot{x} - \dot{x}_d) \\
&+ \left.\frac{\partial N(x, \dot{x}, \sigma_3, 0, 0, 0, \dddot{x}_d)}{\partial \sigma_3}\right|_{\sigma_3 = v_3} (\ddot{x} - \ddot{x}_d) \\
&+ \left.\frac{\partial N(x, \dot{x}, \ddot{x}, \sigma_4, 0, 0, \dddot{x}_d)}{\partial \sigma_4}\right|_{\sigma_4 = v_4} (e_1 - 0) \\
&+ \left.\frac{\partial N(x, \dot{x}, \ddot{x}, e_1, \sigma_5, 0, \dddot{x}_d)}{\partial \sigma_5}\right|_{\sigma_5 = v_5} (e_2 - 0) \\
&+ \left.\frac{\partial N(x, \dot{x}, \ddot{x}, e_1, e_2, \sigma_6, \dddot{x}_d)}{\partial \sigma_6}\right|_{\sigma_6 = v_6} (r - 0)
\end{aligned} \tag{149}$$

where $v_1 \in (x_d, x)$, $v_2 \in (\dot{x}_d, \dot{x})$, $v_3 \in (\ddot{x}_d, \ddot{x})$, $v_4 \in (0, e_1)$, $v_5 \in (0, e_2)$, and $v_6 \in (0, r)$. The right-hand side of (149) can be upper bounded as follows

$$
\begin{aligned}
\tilde{N} \leq\ & \left\|\left.\frac{\partial N(\sigma_1, \dot{x}_d, \ddot{x}_d, 0, 0, 0, \dddot{x}_d)}{\partial \sigma_1}\right|_{\sigma_1=v_1}\right\| \|e_1\| \\
& + \left\|\left.\frac{\partial N(x, \sigma_2, \ddot{x}_d, 0, 0, 0, \dddot{x}_d)}{\partial \sigma_2}\right|_{\sigma_2=v_2}\right\| \|\dot{e}_1\| \\
& + \left\|\left.\frac{\partial N(x, \dot{x}, \sigma_3, 0, 0, 0, \dddot{x}_d)}{\partial \sigma_3}\right|_{\sigma_3=v_3}\right\| \|\ddot{e}_1\| \\
& + \left\|\left.\frac{\partial N(x, \dot{x}, \ddot{x}, \sigma_4, 0, 0, \dddot{x}_d)}{\partial \sigma_4}\right|_{\sigma_4=v_4}\right\| \|e_1\| \\
& + \left\|\left.\frac{\partial N(x, \dot{x}, \ddot{x}, e_1, \sigma_5, 0, \dddot{x}_d)}{\partial \sigma_5}\right|_{\sigma_5=v_5}\right\| \|e_2\| \\
& + \left\|\left.\frac{\partial N(x, \dot{x}, \ddot{x}, e_1, e_2, \sigma_6, \dddot{x}_d)}{\partial \sigma_6}\right|_{\sigma_6=v_6}\right\| \|r\| .
\end{aligned}
\tag{150}
$$

The partial derivatives in (150) can be calculated from (147) as

$$\frac{\partial N(\sigma_1, \dot{x}_d, \ddot{x}_d, 0, 0, 0, \dddot{x}_d)}{\partial \sigma_1} = \frac{\partial \bar{M}(\sigma_1)}{\partial \sigma_1}\dddot{x}_d \tag{151}$$

$$+\frac{\partial \dot{\bar{M}}(\sigma_1, \dot{x}_d)}{\partial \sigma_1}\ddot{x}_d$$

$$+\frac{\partial \dot{\bar{C}}(\sigma_1, \dot{x}_d, \ddot{x}_d)}{\partial \sigma_1}\dot{x}_d$$

$$+\frac{\partial \bar{C}(\sigma_1, \dot{x}_d)}{\partial \sigma_1}\ddot{x}_d$$

$$\frac{\partial N(x, \sigma_2, \ddot{x}_d, 0, 0, 0, \dddot{x}_d)}{\partial \sigma_2} = \frac{\partial \dot{\bar{M}}(x, \sigma_2)}{\partial \sigma_2}\ddot{x}_d \tag{152}$$

$$+\frac{\partial \dot{\bar{C}}(x, \sigma_2, \ddot{x}_d)}{\partial \sigma_2}\sigma_2$$

$$+ \dot{\bar{C}}(x, \sigma_2, \ddot{x}_d)$$

$$+\frac{\partial \bar{C}(x, \sigma_2)}{\partial \sigma_2}\ddot{x}_d$$

$$\frac{\partial N(x, \dot{x}, \sigma_3, 0, 0, 0, \dddot{x}_d)}{\partial \sigma_3} = \dot{\bar{M}}(x, \dot{x}) + \frac{\partial \dot{\bar{C}}(x, \dot{x}, \sigma_3)}{\partial \sigma_3}\dot{x} \tag{153}$$

$$+\bar{C}(x, \dot{x}) + \bar{B}$$

$$\frac{\partial N(x, \dot{x}, \ddot{x}, \sigma_4, 0, 0, \dddot{x}_d)}{\partial \sigma_4} = \alpha_2^3 \bar{M}(x) \tag{154}$$

$$\frac{\partial N(x, \dot{x}, \ddot{x}, e_1, \sigma_5, 0, \dddot{x}_d)}{\partial \sigma_5} = 1 - \alpha_1^2 \bar{M}(x) - \alpha_1\alpha_2 \bar{M}(x) \tag{155}$$

$$-\alpha_2^2 \bar{M}(x)$$

$$\frac{\partial N(x, \dot{x}, \ddot{x}, e_1, e_2, \sigma_6, \dddot{x}_d)}{\partial \sigma_6} = (\alpha_1 + \alpha_2) \bar{M}(x) \tag{156}$$

$$+\frac{1}{2} \dot{\bar{M}}(x, \dot{x}).$$

By noting that

$$
\begin{aligned}
v_1 &= x - c_1 (x - x_d) & v_2 &= \dot{x} - c_2 (\dot{x} - \dot{x}_d) \\
v_3 &= \ddot{x} - c_3 (\ddot{x} - \ddot{x}_d) & v_4 &= e_1 - c_4 (e_1 - 0) \\
v_5 &= e_2 - c_5 (e_2 - 0) & v_6 &= r - c_6 (r - 0)
\end{aligned}
$$

where $c_i \in (0, 1)$ $\forall i = 1, 2, ..., 6$,, if the assumptions stated for the system model and the desired trajectory are met, an upper bound for the right-hand side of (151)-(156) can be written as follows

$$\left\| \frac{\partial N(\sigma_1, \dot{x}_d, \ddot{x}_d, 0, 0, 0, \dddot{x}_d)}{\partial \sigma_1} \right|_{\sigma_1 = v_1} \right\| \leqslant \rho_1(x, \dot{x}, \ddot{x}) \tag{157}$$

$$\left\| \frac{\partial N(x, \sigma_2, \ddot{x}_d, 0, 0, 0, \dddot{x}_d)}{\partial \sigma_2} \right|_{\sigma_2 = v_2} \right\| \leqslant \rho_2(x, \dot{x}, \ddot{x})$$

$$\left\| \frac{\partial N(x, \dot{x}, \sigma_3, 0, 0, 0, \dddot{x}_d)}{\partial \sigma_3} \right|_{\sigma_3 = v_3} \right\| \leqslant \rho_3(x, \dot{x})$$

$$\left\| \frac{\partial N(x, \dot{x}, \ddot{x}, \sigma_4, 0, 0, \dddot{x}_d)}{\partial \sigma_4} \right|_{\sigma_4 = v_4} \right\| \leqslant \rho_4(x)$$

$$\left\| \frac{\partial N(x, \dot{x}, \ddot{x}, e_1, \sigma_5, 0, \dddot{x}_d)}{\partial \sigma_5} \right|_{\sigma_5 = v_5} \right\| \leqslant \rho_5(x)$$

$$\left\| \frac{\partial N(x, \dot{x}, \ddot{x}, e_1, e_2, \sigma_6, \dddot{x}_d)}{\partial \sigma_6} \right|_{\sigma_6 = v6} \right\| \leqslant \rho_6(x, \dot{x})$$

where $\rho_i(\cdot)$ $\forall i = 1, 2, ..., 6$, are positive nondecreasing functions of $x(t)$, $\dot{x}(t)$, and $\ddot{x}(t)$. After substituting (157) into (150), $\tilde{N}(\cdot)$ can be expressed as

$$\begin{aligned}
\tilde{N} \leqslant\ & (\rho_1(\|e_1\|, \|e_2\|, \|r\|) + \rho_4(\|e_1\|)) \|e_1\| \tag{158} \\
& + (\rho_2(\|e_1\|, \|e_2\|, \|r\|)) \|\dot{e}_1\| \\
& + (\rho_3(\|e_1\|, \|e_2\|)) \|\ddot{e}_1\| \\
& + (\rho_5(\|e_1\|)) \|e_2\| \\
& + (\rho_6(\|e_1\|, \|e_2\|)) \|r\|.
\end{aligned}$$

where (16)-(18) were utilized. The expressions in (16) and (72) can now be used to upper bound the right-hand side of (158) as in (76).